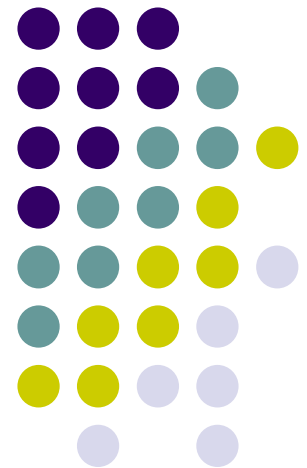# Nonlinear Simulations of Alfvén Eigenmodes destabilized by Energetic Particles
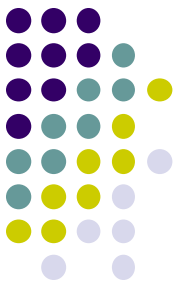
Y. Todo

(National Institute for Fusion Science, Japan)

5th ITER International Summer School

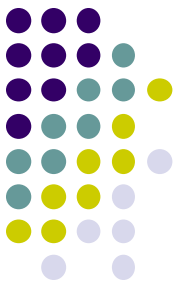(Aix en Provence, France, June 20-24, 2011)

- many thanks to
  - N. Nakajima, A. Ito, T.-H. Watanabe, M. Osakabe, K. Toi, M. Isobe (NIFS)
  - H. Wang [Univ. Advanced Studies (Sokendai)]
  - A. Bierwage, M. Yagi, N. Aiba, K. Shinohara, M. Ishikawa, M. Takechi (JAEA)
  - S. Yamamoto (Kyoto Univ.)
  - H. L. Berk, B. N. Breizman (IFS, Univ. Texas)
  - D. A. Spong (ORNL)
  - C. C. Kim (Univ. Washington)
  - ITPA Energetic Particle Topical Group

Outline
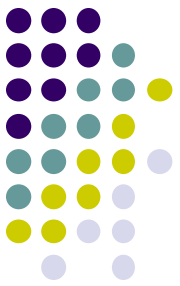
- Introduction
  - Interaction of energetic particles and Alfvén eigenmode in toroidal plasmas
- Simulation models
  - EP + MHD hybrid simulation model
  - Reduced simulation model with constant AE spatial profile
- Simulation of AE bursts
  - Reduced simulation
  - Hybrid simulation with nonlinear MHD effects

Constants of motion in toroidal plamas (1)

- In axisymmetric (independent of toroidal angle φ) equilibrium (time-independent) fields:

  - energy E

  - magnetic moment μ

  - toroidal momentum $P_\varphi = e_h \Psi + m_h R v_\varphi$ are constant along particle orbit
    (Ψ poloidal magnetic flux, e_h and m_h are charge and mass)

Constants of motion in toroidal plamas (2)

- In the presence of a wave with angular frequency ω and toroidal mode number n:

  - μ is conserved if $\omega \ll \Omega_h = e_h B / m_h$
  - neither energy nor toroidal momentum is conserved.
  - however, their combination $E' = E - \omega P_\varphi / n$ is conserved.

E' is conserved during the wave-particle interaction in axisymmetric equilibrium (1)

Energy and toroidal momentum evoution with equilibrium field Hamiltonian H_0 and wave Hamiltonian H_1
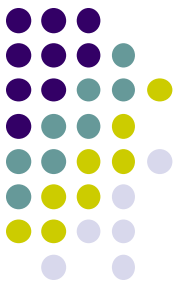
$$\frac{dE}{dt} = \frac{\partial H}{\partial t} = \frac{\partial}{\partial t}\left(H_0 + H_1\right) = \frac{\partial}{\partial t}H_1$$

$$\frac{dP_\varphi}{dt} = -\frac{\partial H}{\partial \varphi} = -\frac{\partial}{\partial \varphi}\left(H_0 + H_1\right) = -\frac{\partial}{\partial \varphi}H_1$$

because $\dfrac{\partial}{\partial t}H_0 = 0$ (equilibrium)

and $\dfrac{\partial}{\partial \varphi}H_0 = 0$ (axisymmetric).
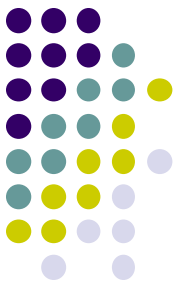
Suppose the wave amplitude is constant,

H_1 is written in cylindrical coordinates (R, φ, z)

$$H_1 = \hat{H}_1(R, z) e^{in\varphi - i\omega t}$$

$$\frac{dE}{dt} = \frac{\partial H_1}{\partial t} = -i\omega \hat{H}_1(R, z) e^{in\varphi - i\omega t}$$

$$\frac{dP_\varphi}{dt} = -\frac{\partial H_1}{\partial \varphi} = -in\hat{H}_1(R, z) e^{in\varphi - i\omega t}$$

Then, $\dfrac{dE'}{dt} = \dfrac{d}{dt}\left(E - \dfrac{\omega}{n} P_\varphi \right) = 0$ is satisfied.

Conservation of E' suggests …

In wave-particle interaction in tokamak plasmas,

the conservation of E' leads to

$$\frac{\delta E}{\omega} = \frac{\delta P_\varphi}{n} \approx \frac{e_h \delta \psi}{n}$$
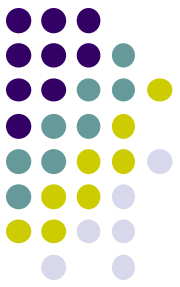
Energy transfer between wave and particle (δE),

and change in poloidal mangetic flux ($\delta \psi$)

(= radial location; spatial transport) are related to each other.

This suggests qualitatively

for high ω (such as ICRF) : δE is important

for low ω and high n (such as ITG) : $\delta \psi$ is important

Why are AE modes destabilized by energetic particles? (1)

Q1 : Can particles interact with ideal MHD modes with $E_{//} = 0$?

A1 : in toroidal plasmas, grad - B and curvature drifts

-> $\mathbf{v}_\perp$ -> energy transfer through $e_h \mathbf{v}_\perp \cdot E_\perp$

Q2 : Slowing down distribution and Maxwell distribution have negative gradient in energy

$$\frac{\partial f}{\partial E} < 0$$

This leads to Landau damping which stabilizes AE modes.

Why are AE modes destabilized by energetic particles? (2)

We should consider the derivative

keeping $E' = E - \dfrac{\omega}{n} P_\varphi = \text{constant},$

$$\left. \frac{\partial f}{\partial E} \right|_{E'} = \frac{\partial f}{\partial E} + \frac{n}{\omega} \frac{\partial f}{\partial P_\varphi}$$

The toroidal momentum is $P_\varphi = e_h \psi + m_h R \text{v}_\varphi.$

If we apporixmate $P_\varphi \cong e_h \psi,$

$$\frac{n}{\omega} \frac{\partial f}{\partial P_\varphi} \cong \frac{n}{\omega} \frac{\partial f}{e_h \partial \psi} = \frac{n}{\omega} \frac{1}{e_h R B_\theta} \frac{\partial f}{\partial r}$$

With $B_\theta = \dfrac{\tau r B}{q R}$ $(B > 0, \ \tau = \text{-1 or 1})$

$$\frac{n}{\omega} \frac{\partial f}{\partial P_\varphi} \cong \frac{n}{\omega} \frac{\tau q}{e_h B} \frac{\partial f}{r \partial r}$$

Why are AE modes destabilized by energetic particles? (3)

Introducing "tempereature" T which replaces energy derivative

$$\frac{\partial f}{\partial E} = -\frac{f}{T}, \text{ and } \omega_* = \frac{\tau q T}{e_h B}\frac{\partial \ln f}{r \partial r} \ ,$$

$$\left.\frac{\partial f}{\partial E}\right|_{E'} = -\frac{f}{T}\left(1 - \frac{n}{\omega}\omega_*\right)$$

When the radial gradient of f is sufficiently large,

the second term $\dfrac{n}{\omega}\omega_*$ makes $\left.\dfrac{\partial f}{\partial E}\right|_{E'} > 0$ to destabilize the AE mode.

This also determines the sign of n/ω, i.e. the toroidal propagation

direction of the AE mode depending on the sign of $\dfrac{\partial f}{\partial r}$.

Why are AE modes destabilized by energetic particles? (4) φ propagation

Toroidal propagation direction of AE modes destabilized by EP spatial gradient can be expressed as follows :

$$\text{sgn}(e_h) \cdot \text{sgn}\left(-\frac{\partial f}{\partial r}\right) \cdot \text{sgn}(B_\theta) = 1 : \text{ propagates } -\varphi \text{ direction}$$
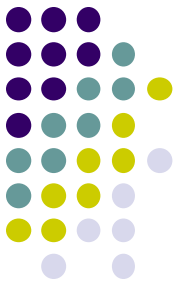
$$\text{sgn}(e_h) \cdot \text{sgn}\left(-\frac{\partial f}{\partial r}\right) \cdot \text{sgn}(B_\theta) = -1 : \text{ propagates } +\varphi \text{ direction}$$

ions : $\text{sgn}(e_h) = 1$, electrons : $\text{sgn}(e_h) = -1$

usually $\text{sgn}\left(-\frac{\partial f}{\partial r}\right) = 1$, but sometimes with ICRH or ECH $\text{sgn}\left(-\frac{\partial f}{\partial r}\right) = -1$

with plama current in $+\varphi$ direction, $\text{sgn}(B_\theta) = -1$

Why are AE modes destabilized by energetic particles? (5) θ propagation

$k_{//} = (mB_\theta / r + nB_\varphi R) / B \approx 0$ gives sign of m/n,

i.e. the poloidal propagation direction.

$\text{sgn}(e_h) \cdot \text{sgn}\left(-\dfrac{\partial f}{\partial r}\right) \cdot \text{sgn}(B_\varphi) = 1:$ propagates $+\theta$ direction

$\text{sgn}(e_h) \cdot \text{sgn}\left(-\dfrac{\partial f}{\partial r}\right) \cdot \text{sgn}(B_\varphi) = -1:$ propagates $-\theta$ direction

The results can be summarized very simply.
AE mode destabilized by EP spatial gradient
rotates in the EP diamagnetic direction.

Why are AE modes destabilized by energetic particles? (6)

For $n = 0$ modes, the energetic particle spatial gradient does not destabilize the AE modes.

However, when f is not isotropic in velocity space and depends on pitch angle variable $\Lambda = \mu B/E$, $f = f(E, \Lambda)$

$$\frac{\partial f}{\partial E} = \left.\frac{\partial f}{\partial E}\right|_{\Lambda} + \frac{\partial \Lambda}{\partial E} \left.\frac{\partial f}{\partial \Lambda}\right|_{E}$$

The second term on the R.H.S. can lead to destabilization of $n = 0$ modes such as GAM.

Outline

- Introduction
  - Interaction of energetic particles and Alfvén eigenmode in toroidal plasmas
- Simulation models
  - EP + MHD hybrid simulation model
  - Reduced simulation model with constant AE spatial profile
- Simulation of AE bursts
  - Reduced simulation
  - Hybrid simulation with nonlinear MHD effects

Initial value codes for AE modes and energetic particles

Method	AE modes	EP	Advantages	Codes
Hybrid simulation	MHD eq.	computatioanl particles (or Vlasov eq. or gyrofluid eq.)	nonlinear MHD effects	M3D TAEFL HMGC MEGA NIMROD
Reduced simulation	AE modes from linear analysis	computational particles (or Vlasov eq.)	reasonable balance between physics contained and demand for comp. resources	ORBIT HAGIS FAC EUTERPE MEGA-R
Gyrokinetic simulation	comp. particles for bulk plasma + GK Poisson eq. and Ampere eq.	computational particles (or Vlasov eq.)	fully kinetic effects	GTC GYGLES GEM GYRO

Guiding center approximation for energetic particles
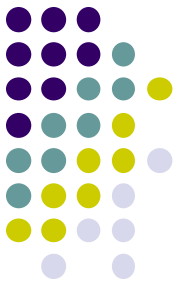
$$\mathbf{u} = \mathbf{v}_{//}^* + \mathbf{v}_E + \mathbf{v}_B$$

$$\mathbf{v}_{//}^* = \frac{v_{//}}{B^*}[\mathbf{B} + \rho_{//} B \nabla \times \mathbf{b}]$$

$$\mathbf{v}_E = \frac{1}{B^*}[\mathbf{E} \times \mathbf{b}]$$

$$\mathbf{v}_B = \frac{1}{q_h B^*}[-\mu \nabla B \times \mathbf{b}]$$

$$\rho_{//} = \frac{m_h v_{//}}{q_h B}$$

$$\mathbf{b} = \mathbf{B}/B$$

$$B^* = B(1 + \rho_{//} \mathbf{b} \cdot \nabla \times \mathbf{b})$$

$$m_h v_{//} \frac{dv_{//}}{dt} = \mathbf{v}_{//}^* \cdot [q_h \mathbf{E} - \mu \nabla B]$$

MHD equations coupled with EP current density

$$\frac{\partial \rho}{\partial t} = -\nabla \cdot (\rho \mathbf{v})$$

$$\rho \frac{\partial}{\partial t} \mathbf{v} = -\rho \vec{\omega} \times \mathbf{v} - \rho \nabla (\frac{v^2}{2}) - \nabla p + (\mathbf{j} - \mathbf{j}'_h) \times \mathbf{B} + \nu \rho [\frac{4}{3} \nabla (\nabla \cdot \mathbf{v}) - \nabla \times \vec{\omega}]$$

$$\frac{\partial \mathbf{B}}{\partial t} = -\nabla \times \mathbf{E}$$

$$\frac{\partial p}{\partial t} = -\nabla \cdot (p \mathbf{v}) - (\gamma - 1) p \nabla \cdot \mathbf{v} + (\gamma - 1)[\nu \rho \omega^2 + \frac{4}{3} \nu \rho (\nabla \cdot \mathbf{v})^2 + \eta \mathbf{j} \cdot (\mathbf{j} - \mathbf{j}_{eq})]$$

$$\mathbf{E} = -\mathbf{v} \times \mathbf{B} + \eta (\mathbf{j} - \mathbf{j}_{eq})$$

$$\mathbf{j} = \frac{1}{\mu_0} \nabla \times \mathbf{B}$$

$$\vec{\omega} = \nabla \times \mathbf{v}$$
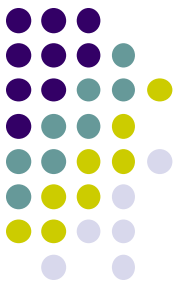
EP current density

Energetic ion current density without ExB drift:

$$\mathbf{j}'_h = \int q_h (\mathbf{v}^*_{//} + \mathbf{v}_B) f d^3v - \nabla \times \int \mu f \mathbf{b} d^3v$$

parallel + curvature drift + grad-B drift   magnetization current

When we neglect $B^* = B(1 + \rho_{//}\mathbf{b} \cdot \nabla \times \mathbf{b})$ in the drift kinetic equations,

$$\mathbf{j}'_h = \mathbf{j}_{h//} + \frac{1}{B}\left(P_{h//}\nabla \times \mathbf{b} - P_{h\perp}\nabla \ln B \times \mathbf{b}\right) - \nabla \times \left(\frac{P_{h\perp}}{B}\mathbf{b}\right).$$

If the energetic particle distribution is isotropic ($P_{h//} = P_{h\perp} \equiv P_h$),
$-\mathbf{j}'_h \times \mathbf{B}$ term in the MHD momentum equation is reduced to
the pressure gradient, i.e., $-\mathbf{j}'_h \times \mathbf{B} = -\nabla P_h$

The δf method

The energetic ion pressures are calculated using the particle weight :

$$P_{h//}(\mathbf{x}) = P_{h//0}(\mathbf{x}) + \sum_{i}^{N} m_h v_{//i}^2 w_i S(\mathbf{x} - \mathbf{x}_i) \ ,$$

$$P_{h\perp}(\mathbf{x}) = P_{h\perp 0}(\mathbf{x}) \frac{B(\mathbf{x})}{B_0(\mathbf{x})} + B(\mathbf{x}) \sum_{i}^{N} \mu_i w_i S(\mathbf{x} - \mathbf{x}_i) \ .$$

The evolution of the particle weight is given by,

$$\frac{d}{dt} w_i = -\alpha V_i \frac{d}{dt} f_0(E,\mu,P_\varphi) = -\alpha V_i \left[\frac{dE}{dt} \frac{\partial f_0}{\partial E} + \frac{dP_\varphi}{dt} \frac{\partial f_0}{\partial P_\varphi} \right]$$

$[\alpha : \text{normalization factor},$

$V_i : \text{phase space volume which the i-th particle occupies}]$

Example of TAE mode (1)
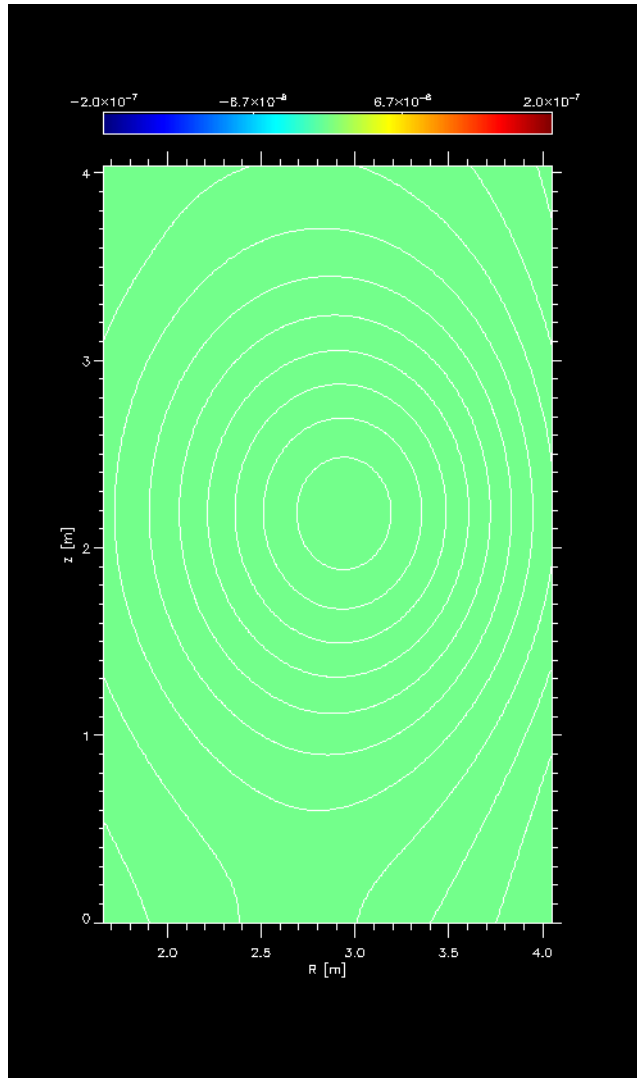
n=3 mode, E_φ

MEGA results on ITPA
linear code benchmark
case [JET shot 77788
(t=44.985s) P. Lauber]

Example of TAE mode (2): in LHD
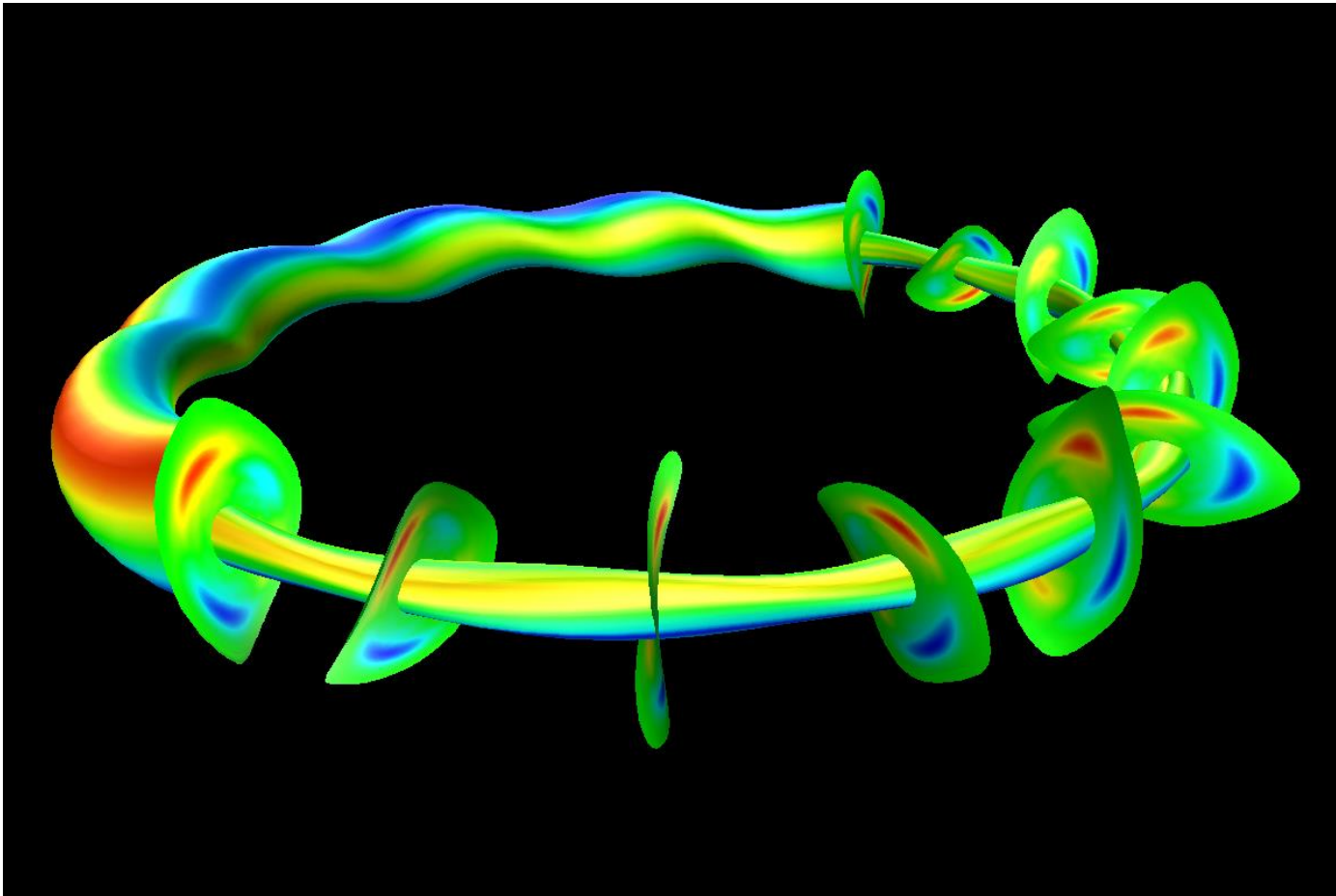
n=1 mode rv_r

MEGA results on LHD shot #47645

Vlasov-MHD simulation of AE evolution

[Y. Todo et al., Phys. Plasmas 2, 2711 (1995)]

- Linear growth and saturation of AE instability

- Amplitude oscillation takes place after the saturation
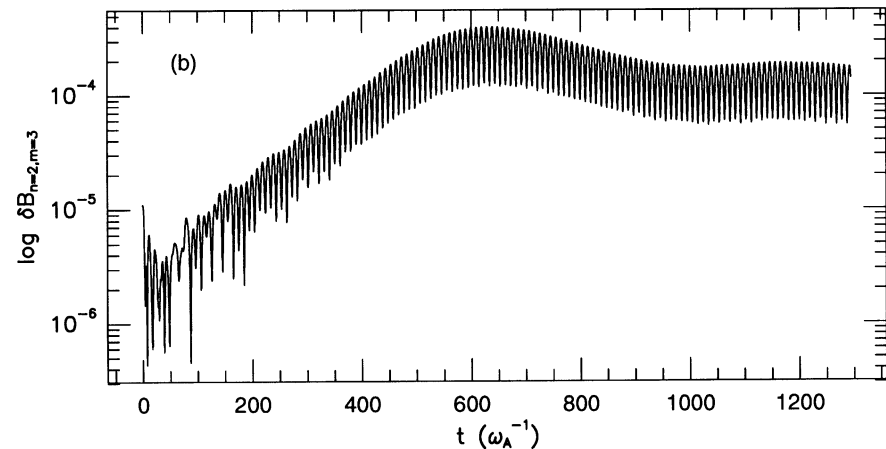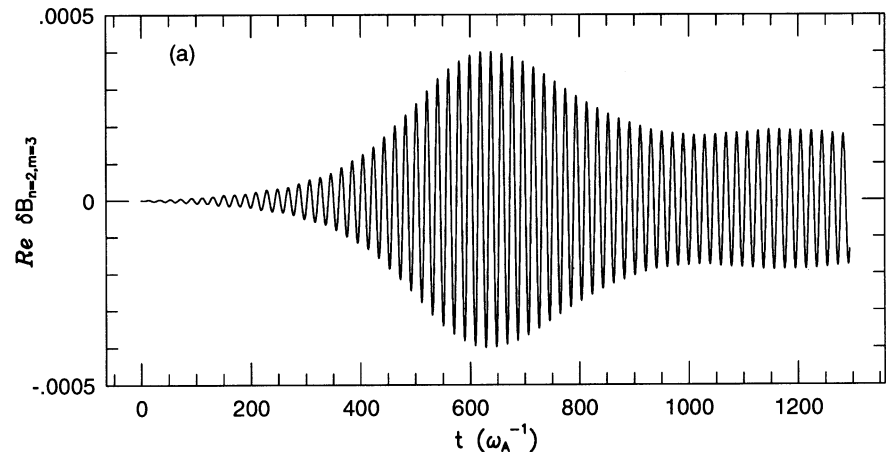
Particle trapping by the Alfvén eigenmode saturates the instability
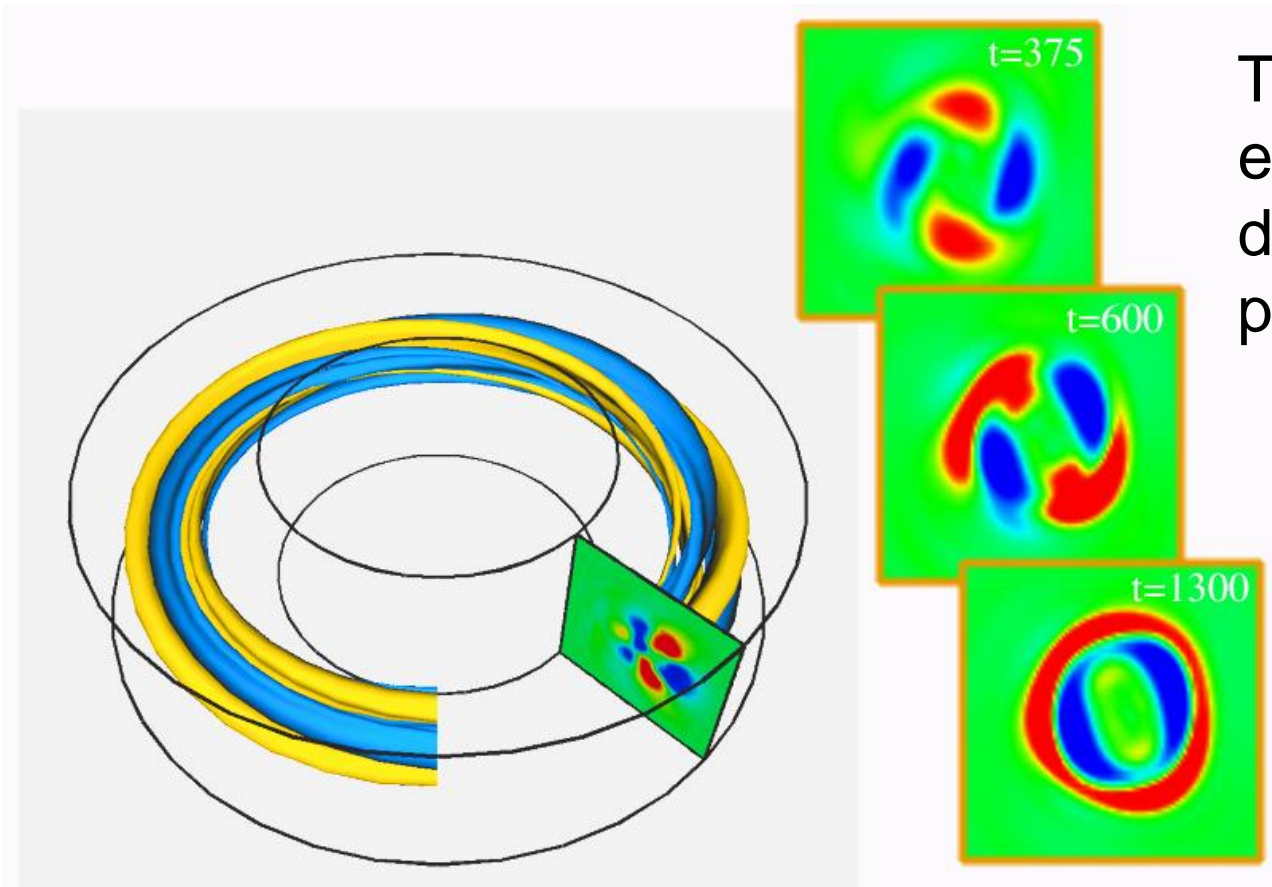
Time evolution of energetic-ion distribution in a poloidal plane

AE spatial profile

Comparison of RSAE and TAE
[H. Wang, poster session]

Figure 8: *The energetic particle perturbation density profiles.*

Figure 3: *The mode profiles of RSAE (left) and TAE (right).*

RSAE interacts primarily only with co- or counter-going particles, while the TAE interacts with both.

Fast Frequency Sweeping mode & ALE in JT-60U (1)
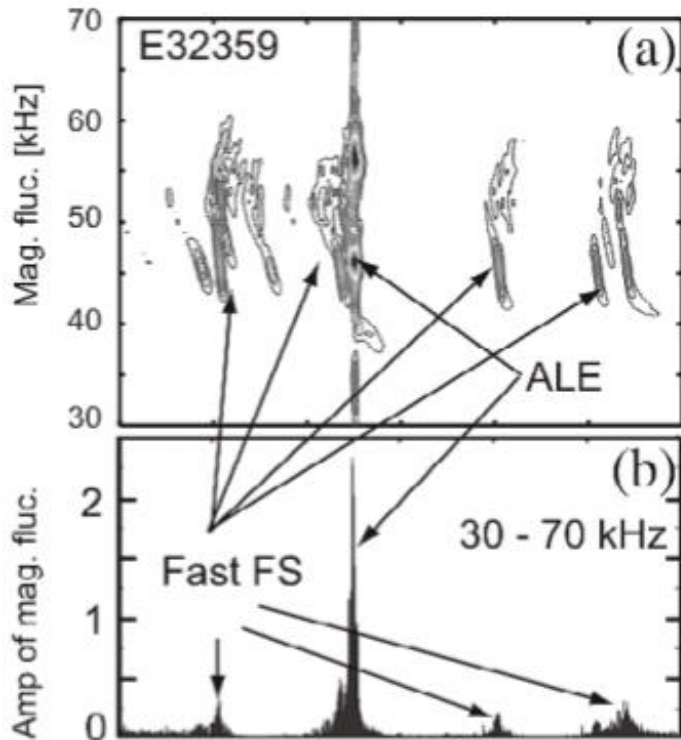
[Shinohara, J. Plasma Fusion Res. 81, 547 (2005)]
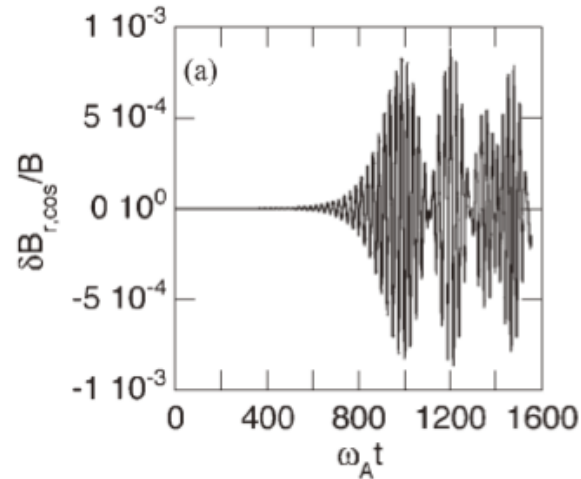
MEGA result.
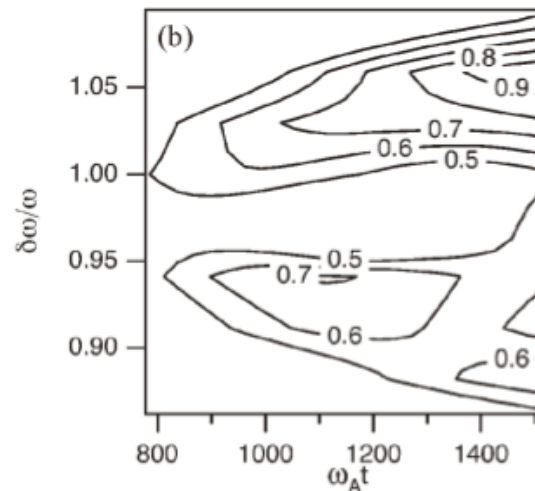
Frequency sweeping rate is comparable to the FFS mode.

[Todo, J. Plasma Fusion Res. 83, 900 (2007)]

Fast Frequency Sweeping mode & ALE in JT-60U (2)

E32359

(a)

ALE

(b)

Fast FS

30 - 70 kHz

shaped

linear, $t=150\omega_{A0}^{-1}$

(c)

linear mode

shaped

(l)

(c)

shaped

$\Delta n_H(t=650,150) / n_{H0}$

(b)
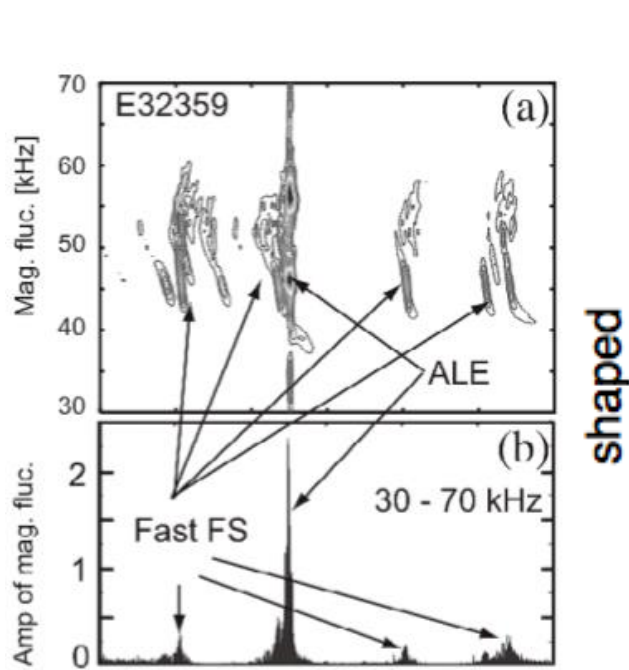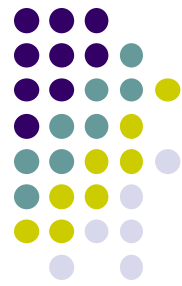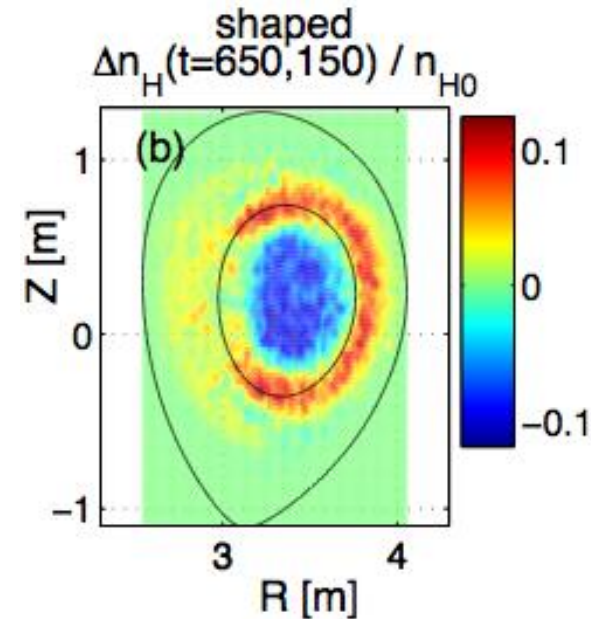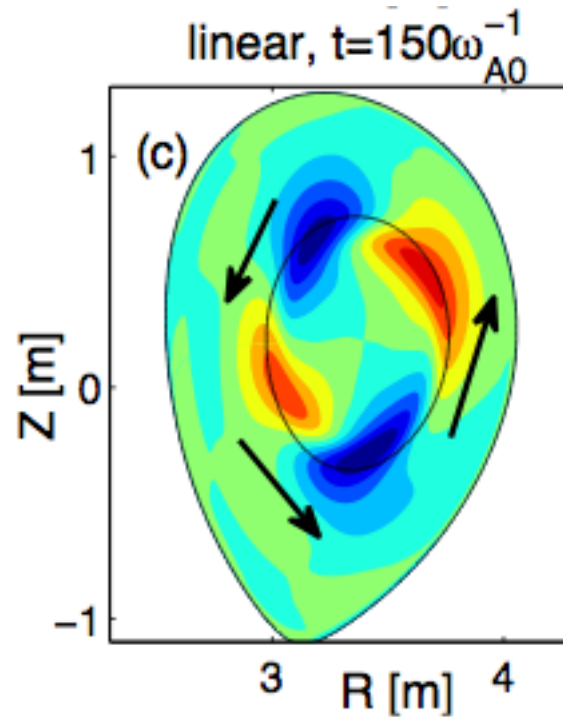
[Shinohara, J. Plasma Fusion Res. 81, 547 (2005)]

ALE was also simulated with HMGC [Briguglio, Phys. plasmas 14, 055904 (2007)].
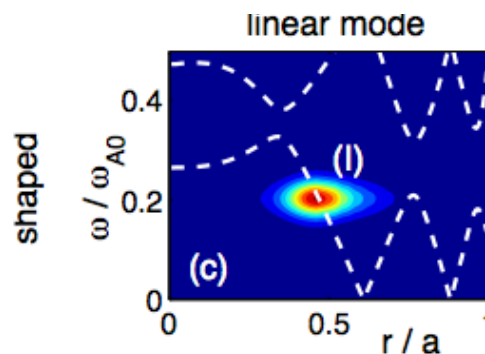
EP redistribution is comparable to the experiment measurement.

[Bierwage, Plasma Fusion Res. (2011)][27]

Simulation of ITER weakly reversed shear plasma

- Low-n (n=2-5) toroidal Alfven eigenmodes (TAE) were found to be unstable.

- Saturation level: $\delta B/B \sim 10^{-3}$

- Redistribution of a particle pressure is 5% of the central value.

- An extended MHD model was employed. Further development is under way.

Toroidal electric field of the n=3 TAE.
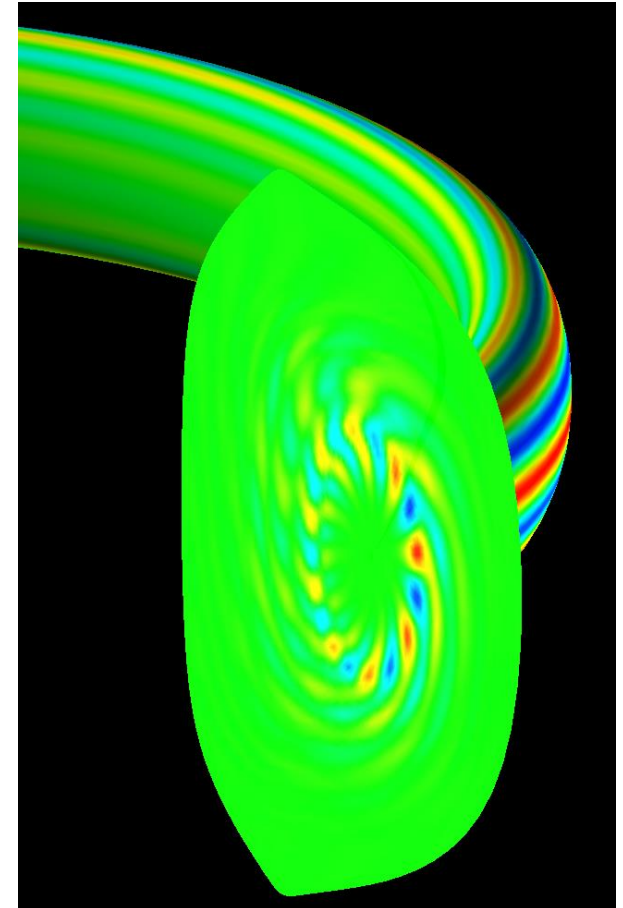
[Y. Todo, J. Plasma Phys. 72, 817 (2006)]

Outline

- Introduction
  - Interaction of energetic particles and Alfvén eigenmode in toroidal plasmas
- Simulation models
  - EP + MHD hybrid simulation model
  - Reduced simulation model with constant AE spatial profile
- Simulation of AE bursts
  - Reduced simulation
  - Hybrid simulation with nonlinear MHD effects

Model of electromagnetic field

$$\Phi_s(R,\varphi,z) = X\sum_m \phi_m(r)\sin(n\varphi + m\vartheta - \omega t),$$

$$\Phi_c(R,\varphi,z) = Y\sum_m \phi_m(r)\cos(n\varphi + m\vartheta - \omega t),$$

$$\Phi = \Phi_s + \Phi_c,$$

$$A_{\|s}(R,\varphi,z) = X\sum_m a_{\|m}(r)\sin(n\varphi + m\vartheta - \omega t),$$

$$A_{\|c}(R,\varphi,z) = Y\sum_m a_{\|m}(r)\cos(n\varphi + m\vartheta - \omega t),$$

$$A_{\|} = A_{\|s} + A_{\|c},$$

$$a_{\|m} = \phi_m(n - m/q)/\omega R_0$$

$$\mathbf{E}_{s(c)} = -\nabla_{\perp}\Phi_{s(c)},$$

$$\mathbf{B}_{s(c)} = \nabla_{\perp}\times(A_{\|s(c)}\mathbf{b})$$
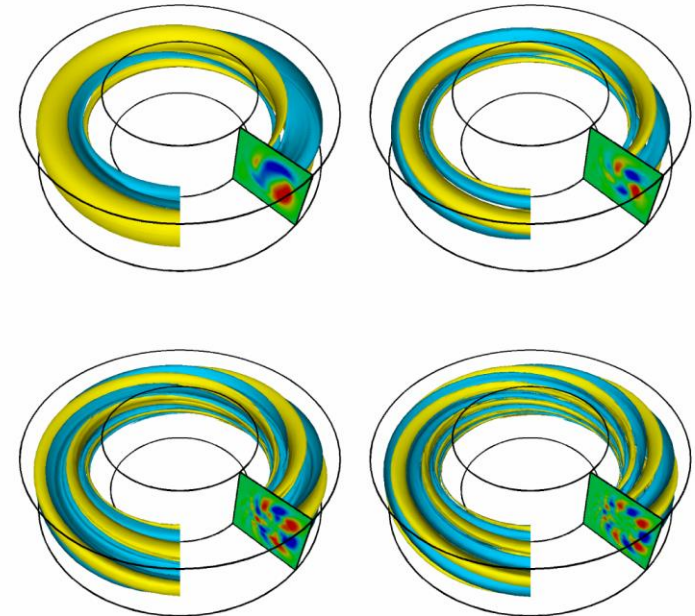
･Spatial profiles and real frequencies of eigenmodes are given in advance of the simulation.

･Amplitude evolution of sine part and cosine part of each eigenmode is calculated independently.

Time evolution of eigenmode

$$\frac{dX}{dt} = \left[-\left\langle \mathbf{j}_f \cdot \mathbf{E}_s \right\rangle \middle/ 2W_s - \gamma_d \right] X,$$

$$\frac{dY}{dt} = \left[-\left\langle \mathbf{j}_f \cdot \mathbf{E}_c \right\rangle \middle/ 2W_c - \gamma_d \right] Y,$$

$$\mathbf{j}_f = \sum_i w_i \frac{m_f V_i^2 (1 + \lambda_i^2)}{2B_0 R_0} \hat{z}$$

$$W_{s(c)} = \left\langle \frac{1}{2\mu_0} \mathbf{B}_{s(c)}^2 + \frac{1}{2\mu_0 V_A^2} \mathbf{E}_{s(c)}^2 \right\rangle$$

similarity to the Interaction Representation of quantum mechanics

Similar to [H.L.Berk, B.N.Breizman, and M.S.Pekker, Nucl. Fusion 35, 1713 (1995)].

The time step is not limited by the AE oscillation period.
It is limited by the growth or damping rate.
(It is limited by the particle orbit integration.)

Outline

- Introduction
  - Interaction of energetic particles and Alfvén eigenmode in toroidal plasmas
- Simulation models
  - EP + MHD hybrid simulation model
  - Reduced simulation model with constant AE spatial profile
- Simulation of AE bursts
  - Reduced simulation
  - Hybrid simulation with nonlinear MHD effects

Alfvén Eigenmode Bursts
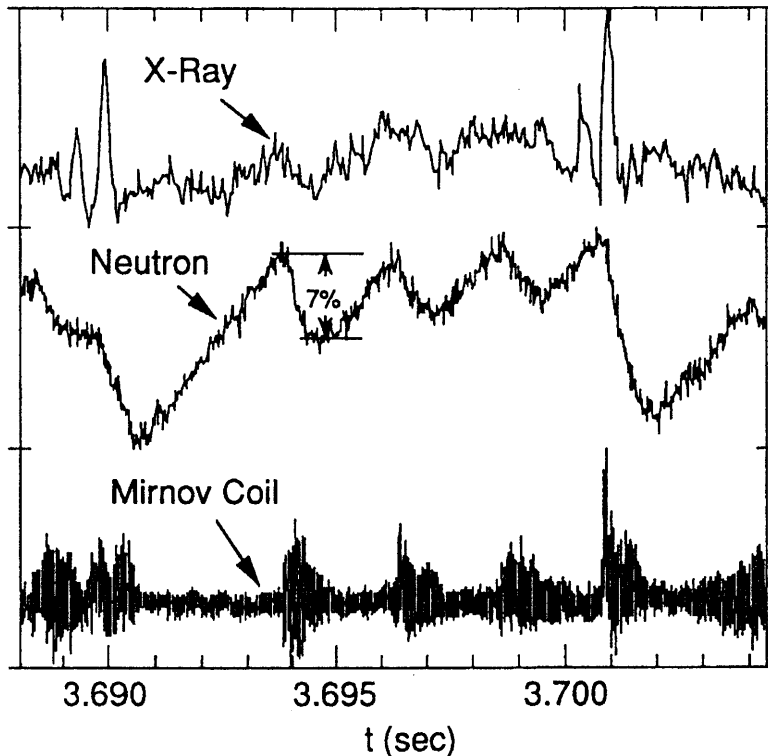
Results from a TFTR experiment [K. L. Wong et al., Phys. Rev. Lett. 66, 1874 (1991).]

Neutron emission: nuclear reaction of thermal D and energetic beam D -> drop in neutron emission = energetic-ion loss

Mirnov coil signal: magnetic field fluctuation -> Alfvén eigenmode bursts

• Alfvén eigenmode bursts take place with a roughly constant time interval.
• 5-7% of energetic beam ions are lost at each burst.

Time evolution of TAE mode amplitude and stored beam energy
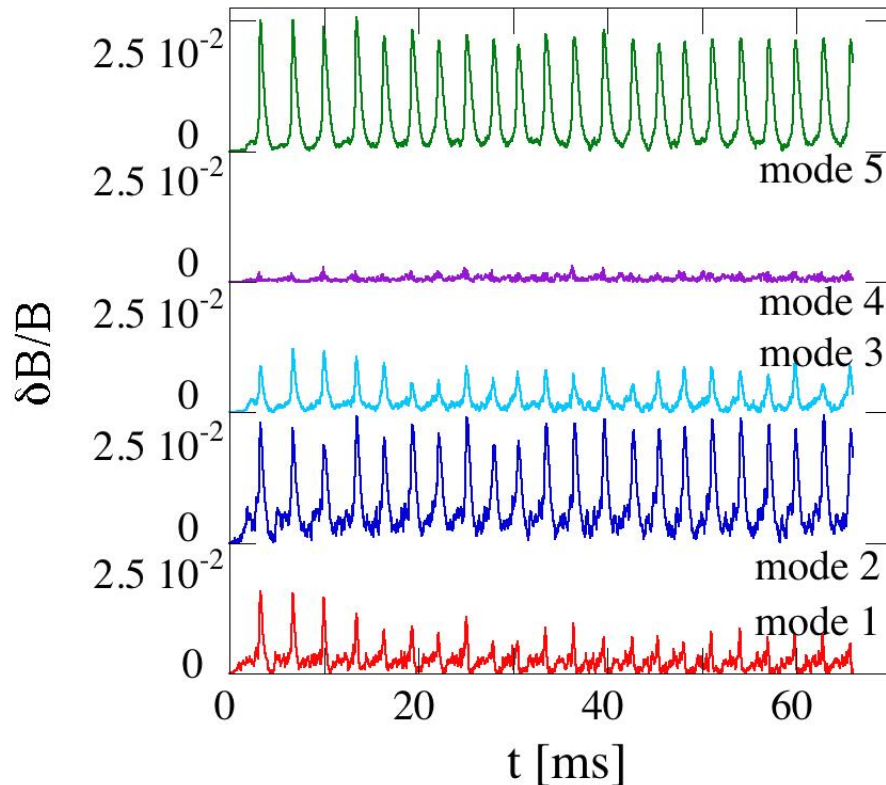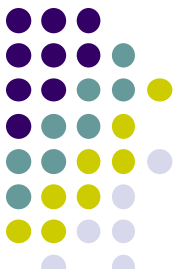
Synchronization of multiple modes due to resonance overlap (left).
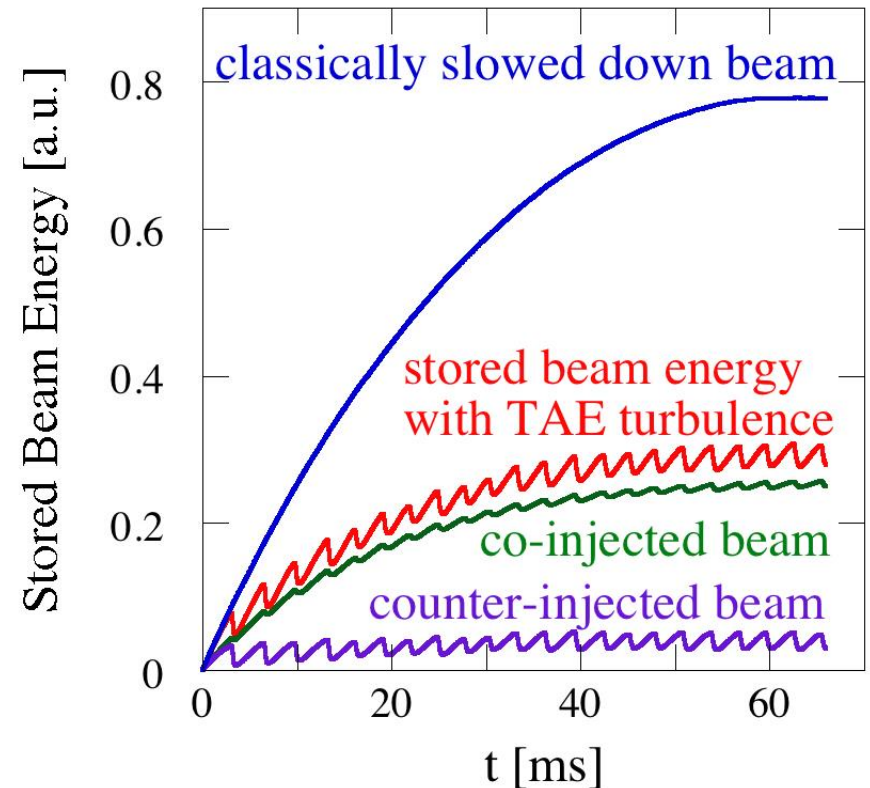
Stored beam energy is reduced to 40% of the classically expected level (right).

The losses balances with the beam injection when the amplitude of the outermost mode reaches to 6x10^{-3}
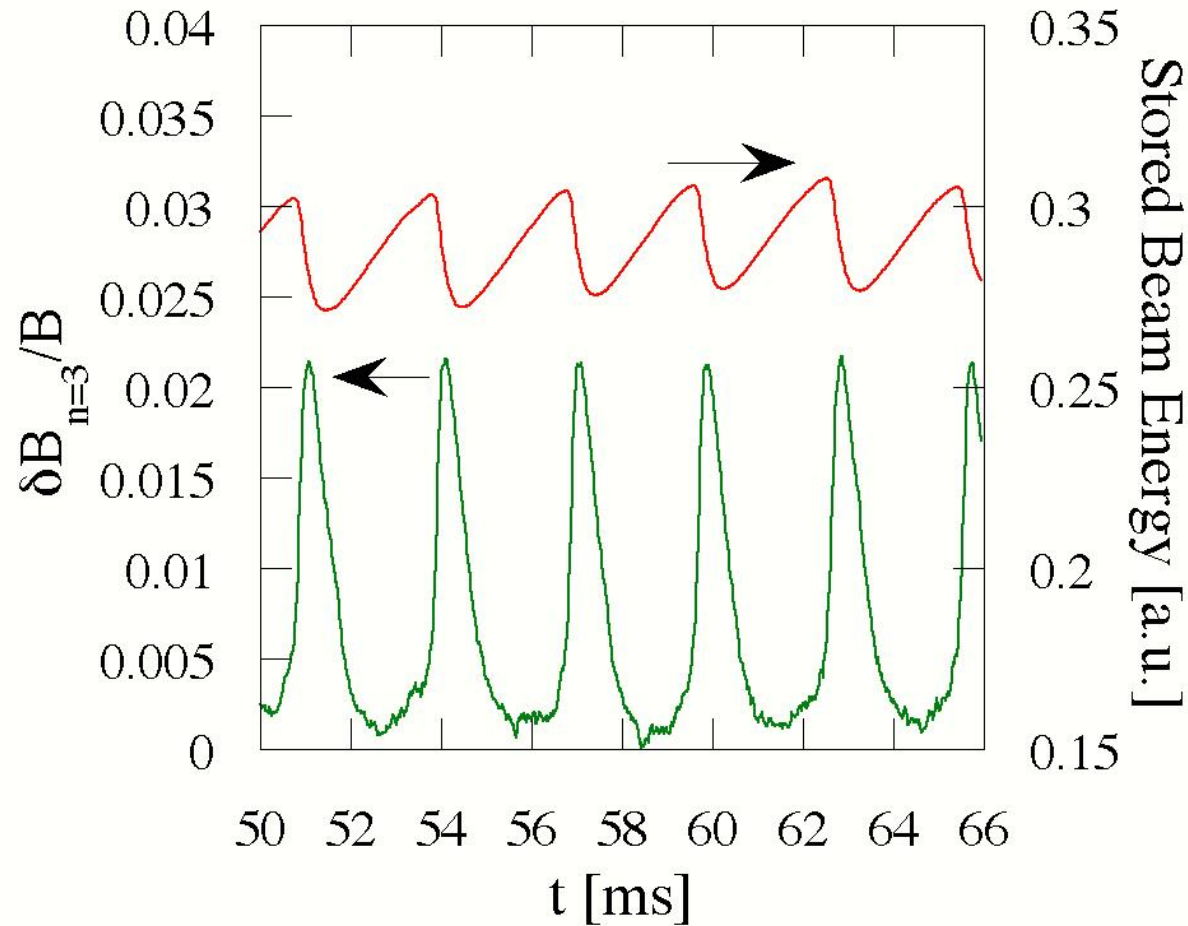
Poincaré plot of energetic-ion orbits in the presence of an AE with constant amplitude ($\delta B/B = 2 \times 10^{-3}$ at the peak)
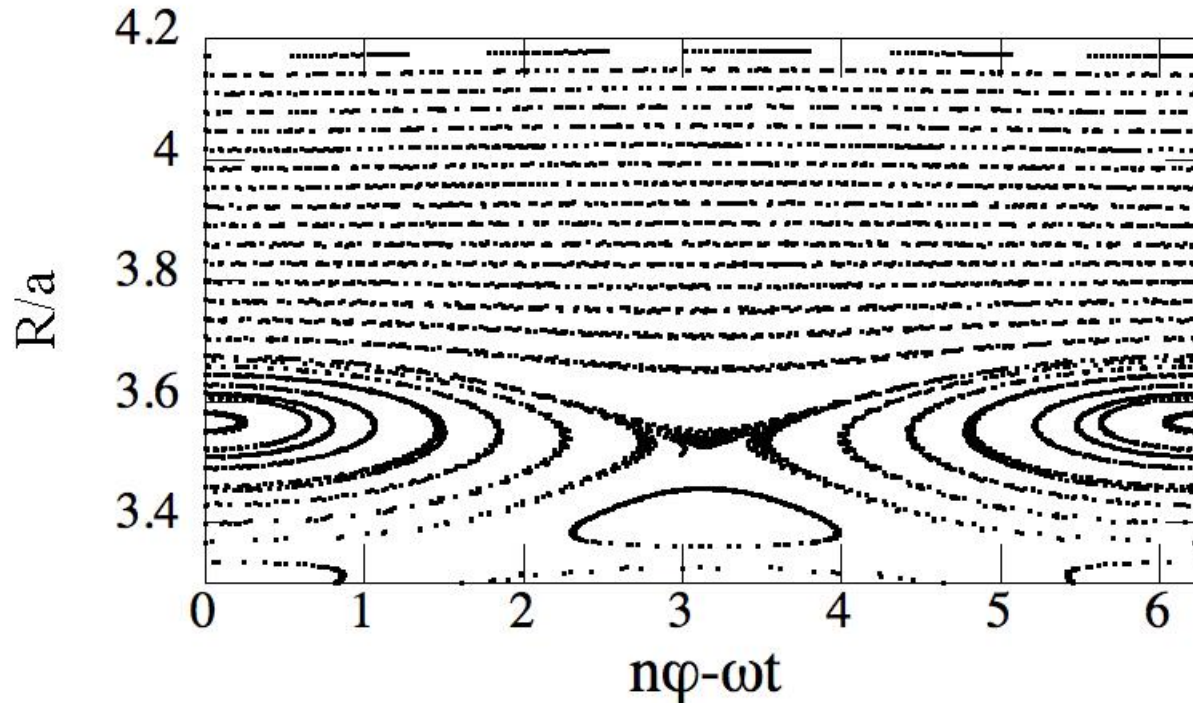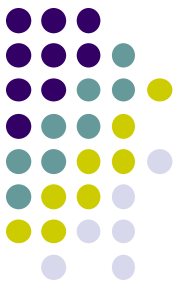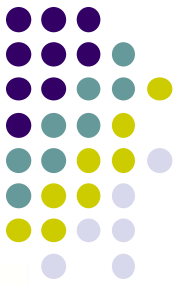

- An island structure is formed in the phase space.
- This is the region of particles trapped by the AE.

Poincaré plots when particle loss balances the injection: resonance overlap of multiple modes takes place
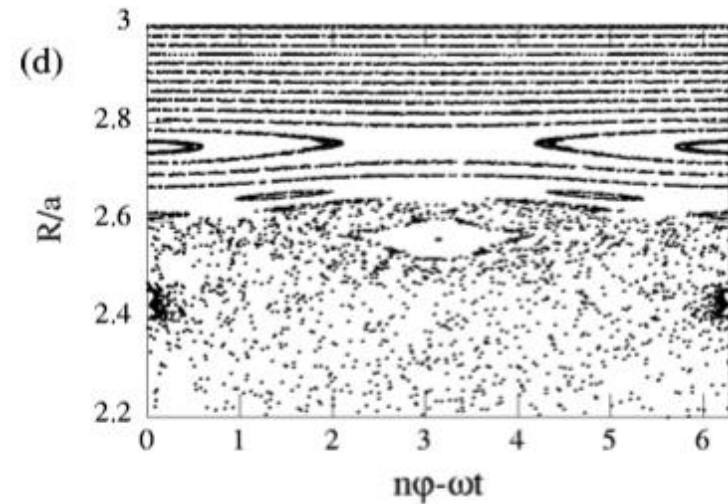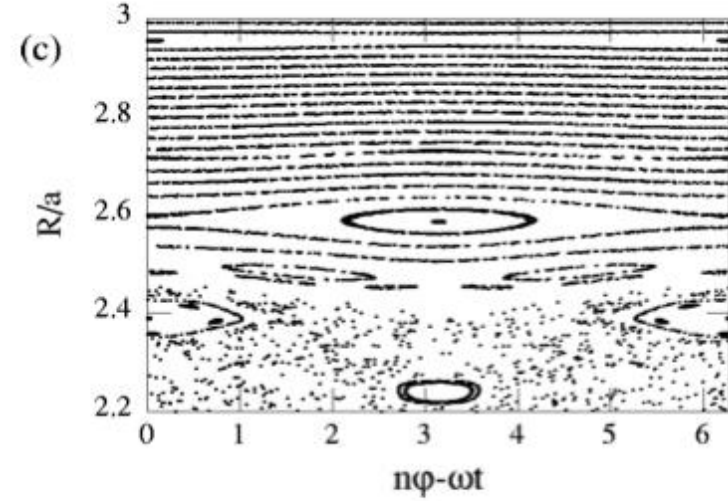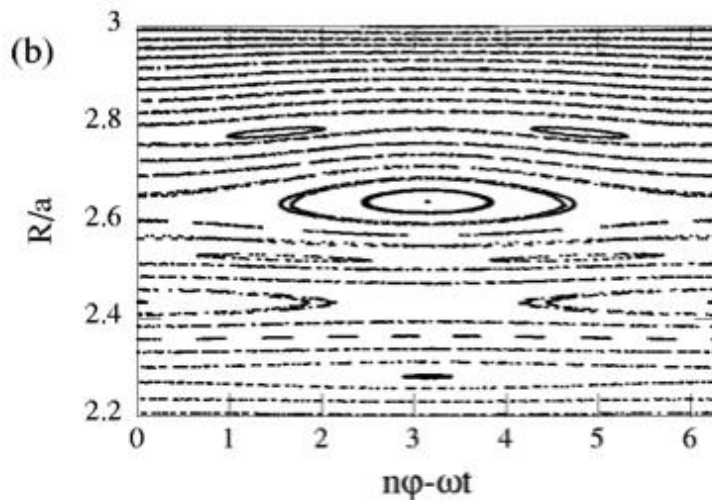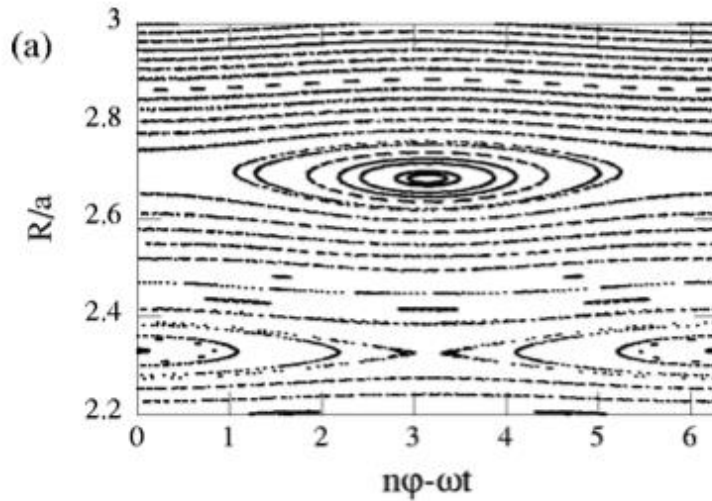
Why do the stochastic regions appear for a single mode?

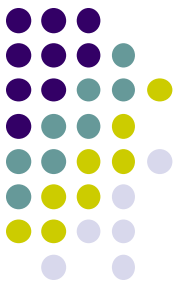(e) n=3 $\delta B/B = 1 \times 10^{-3}$

island structure due to the nonlinear resonances
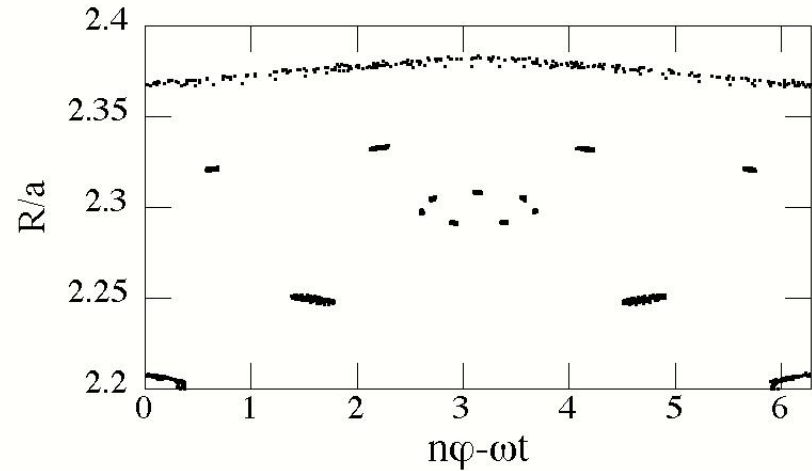
(e) n=3 $\delta B/B = 2 \times 10^{-3}$

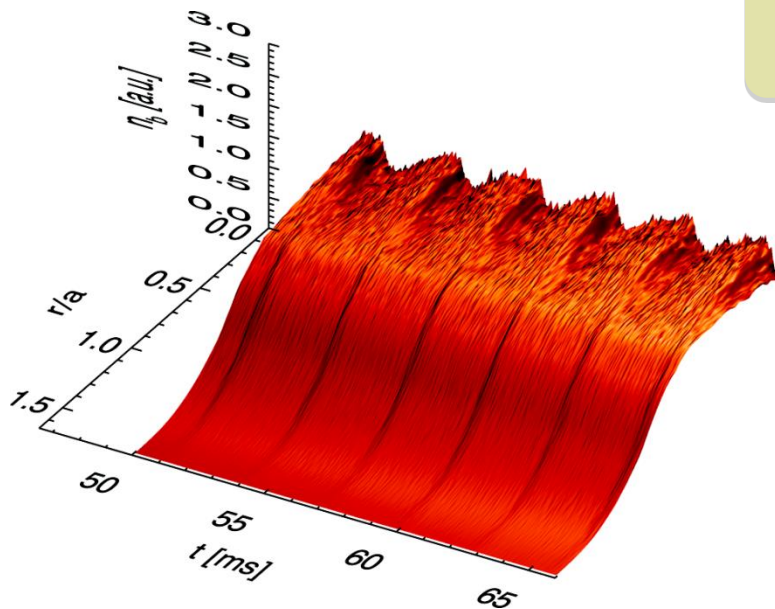KAM surfaces disappear due to the overlap of the nonlinear islands
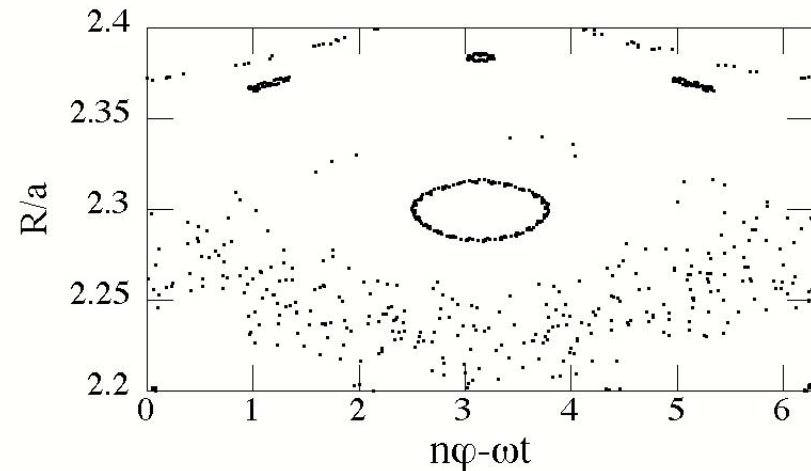
Reduced Simulation of Alfvén Eigenmode Bursts

[Todo, Berk, Breizman, PoP **10**, 2888 (2003)]

• Nonlinear simulation in an open system: **NBI, collisions, losses**

• The TAE bursts in a TFTR experiment [Wong et al. PRL **66**, 1874 (1991)] were reproduced quantitatively.

Time evolution of energetic-ion density profile.

Store of energetic ions

Destabilization of AEs

Transport and loss of energetic ions

Stabilization of AEs
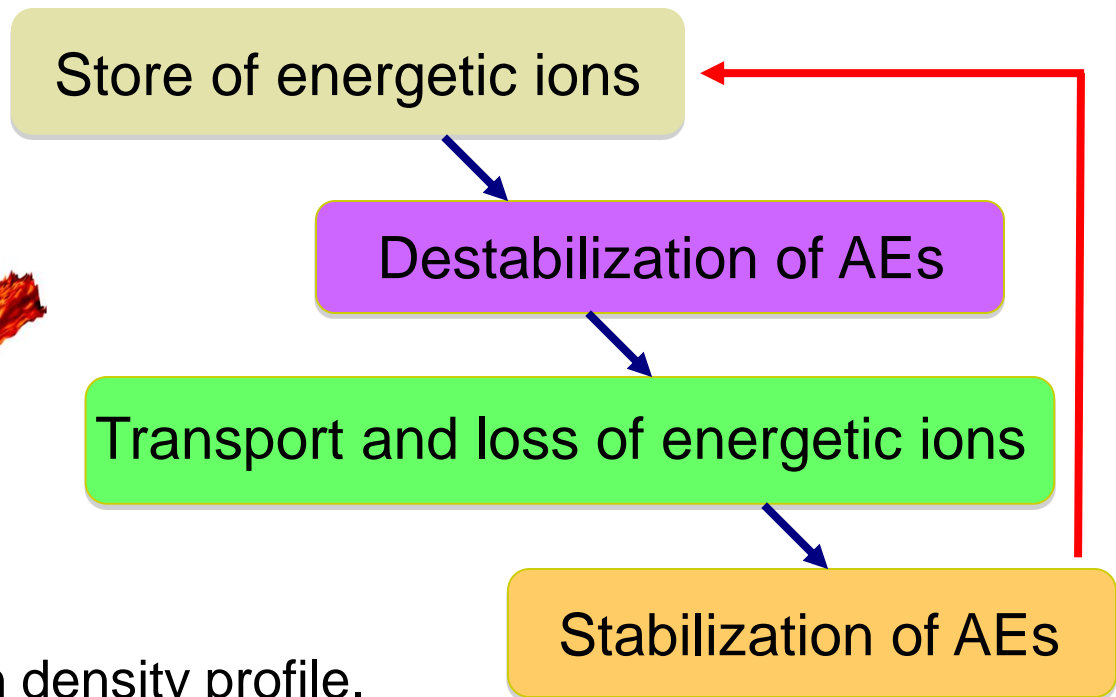
# Summary of the reduced simulation of AE bursts

- consistent with the experiment:
  - synchronization of multiple TAE modes
  - drop in stored beam energy at each burst
  - burst time interval
- inconsistent in saturation amplitude
  - simulation: $\delta B/B \sim 2 \times 10^{-2}$
  - inferred from the plasma displacement at the edge region [Durst et al., PoF B **4**, 3707 (1992)]: $\delta B/B \sim 10^{-3}$

Outline

- Introduction
  - Interaction of energetic particles and Alfvén eigenmode in toroidal plasmas
- Simulation models
  - EP + MHD hybrid simulation model
  - Reduced simulation model with constant AE spatial profile
- Simulation of AE bursts
  - Reduced simulation
  - Hybrid simulation with nonlinear MHD effects

Initial plasma profile and numerical conditions
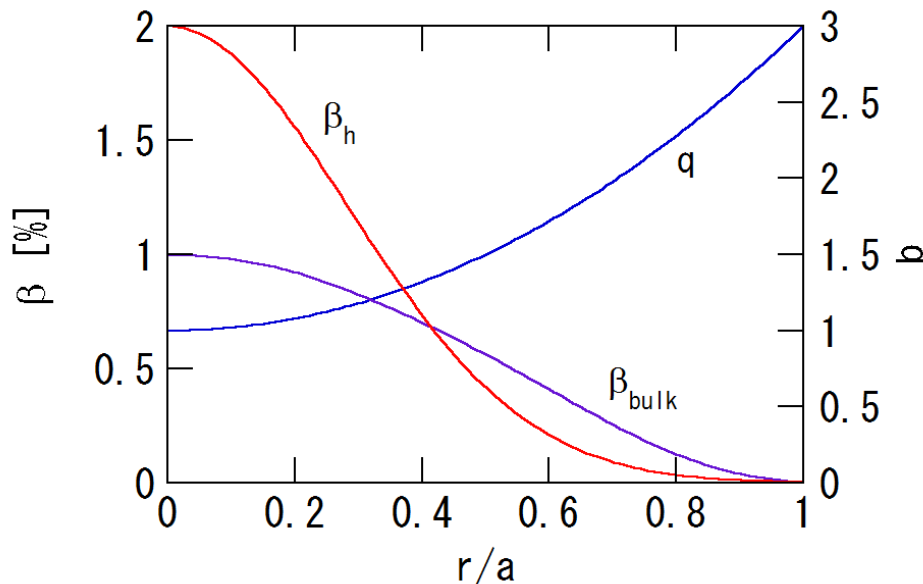
$$\beta_h = \beta_{h0} \exp[-(r/0.4a)^2]$$
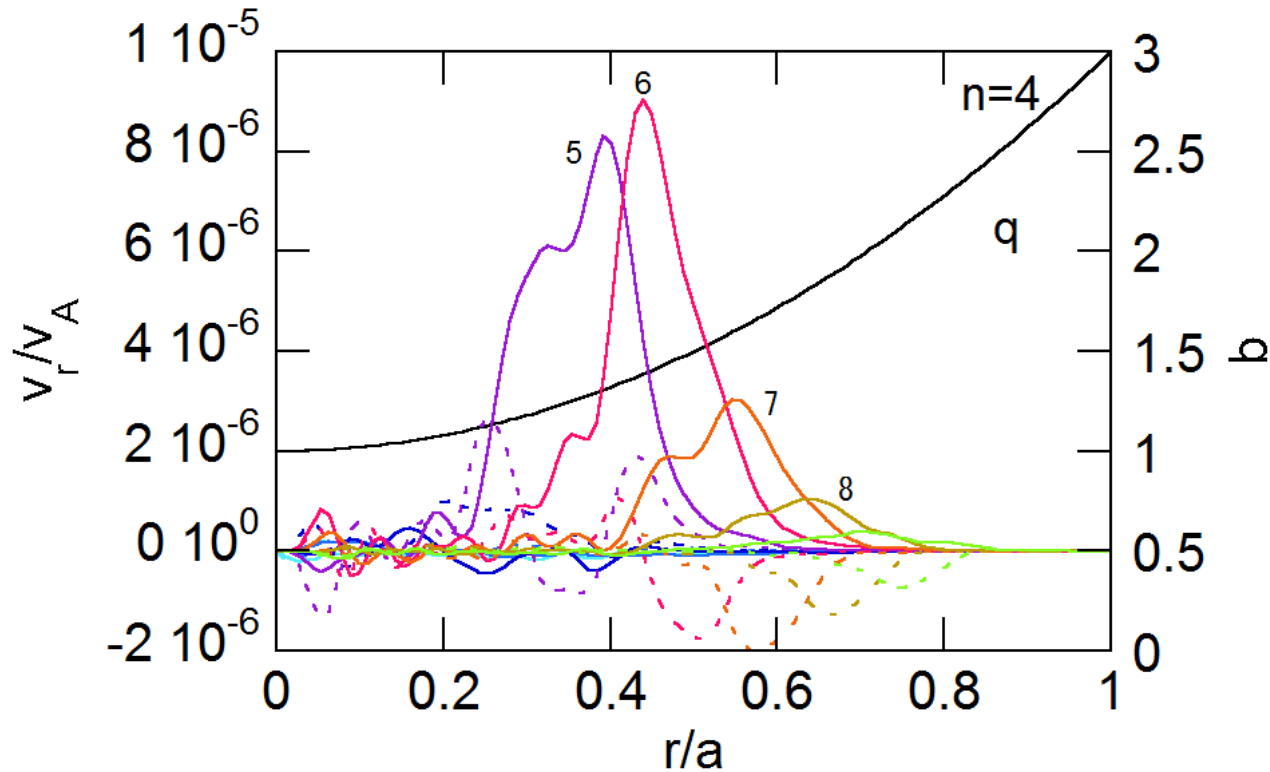
$$q = 1 + 2(r/a)^2$$

$$a\Omega_h / v_A = 16$$

$$R_0 / a = 3.2$$

$$v_b = 1.2 v_A \,, \; v_c = 0.5 v_A$$

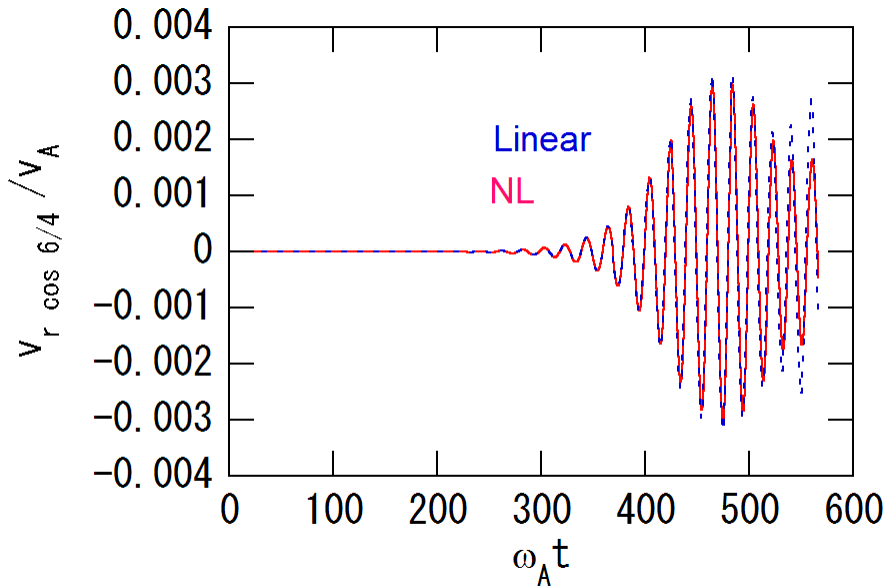Initial energetic-particle distribution: slowing down distribution isotropic in velocity space

The viscosity and resistivity are $\nu = \nu_n = 10^{-6} v_A R_0$ and $\eta = 10^{-6} \mu_0 v_A R_0$. The numbers of grid points are (128, 64, 128) for (R, φ, z). The number of marker particles is 5.2×10^5. $0 \le \varphi \le \pi/2$ for the n=4 mode.

TAE spatial profile (n=4)

The main harmonics are m=5 and 6.

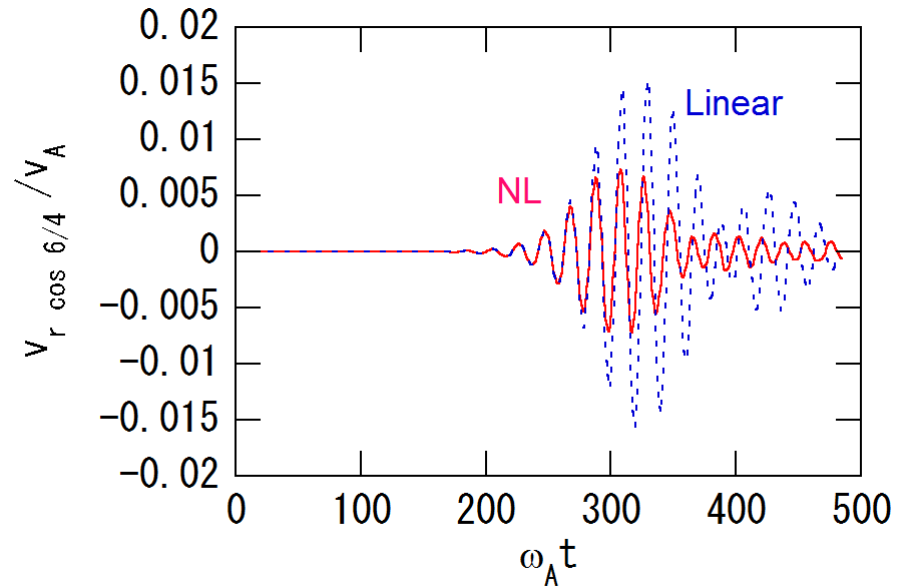# Comparison of linear and NL runs

$\beta_{h0}=1.5\%$
Sat. Level (linear) ~ 3×10^{-3}
Sat. Level (NL)   ~ 3×10^{-3}

$\beta_{h0}=2.0\%$
Sat. Level (linear) ~ 1.6×10^{-2}
Sat. Level (NL)   ~ 8×10^{-3}

The saturation level is reduced to half
in the nonlinear run.

44

Analysis of dissipation from each toroidal mode number

Energy of each toroidal mode number n (n=0, 4, 8, 12, 16)

$$E_n \equiv \frac{1}{2} \int \left(\rho_{n=0} \mathbf{v}_n^2 + (\mathbf{B} - \mathbf{B}_{eq})_n^2 \right) dV$$

Energy dissipation of each toroidal mode number n (n=0, 4, 8, 12, 16)

$$D_n \equiv \int \left[\nu \rho_{n=0} \omega_n^2 + \frac{4}{3} \nu \rho_{n=0} (\nabla \cdot \mathbf{v}_n)^2 + \eta \mathbf{j}_n \cdot (\mathbf{j} - \mathbf{j}_{eq})_n \right] dV$$
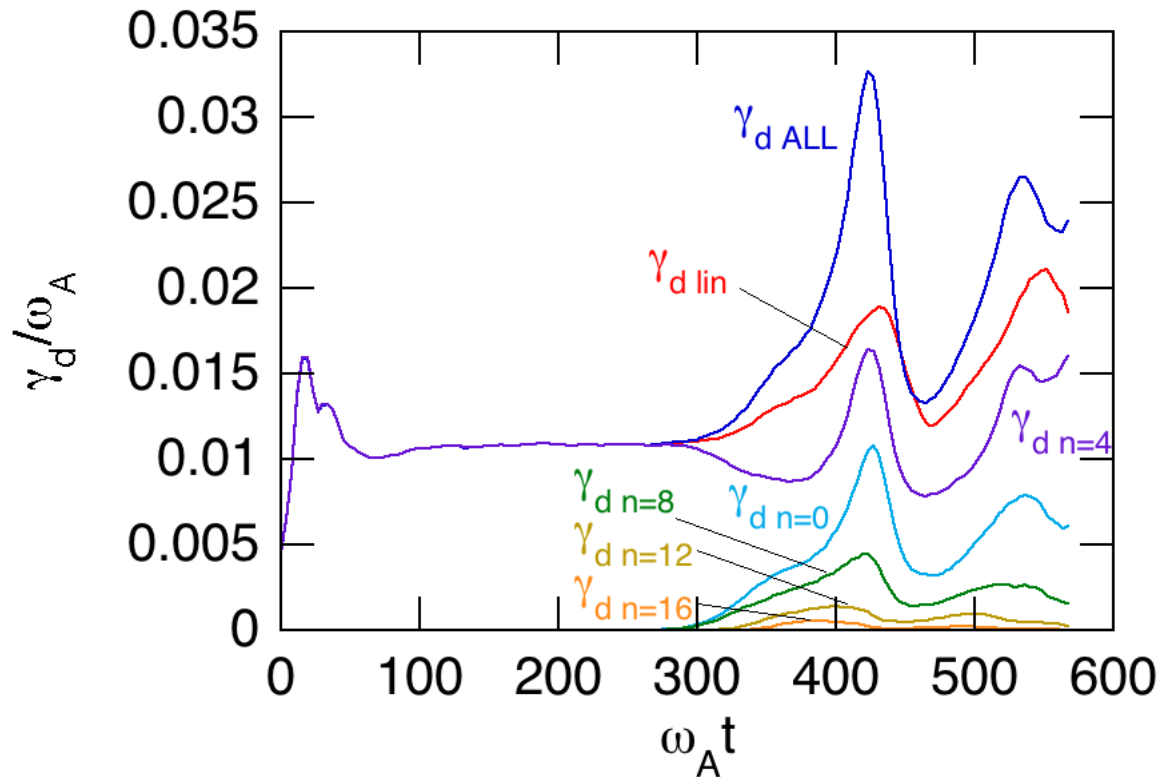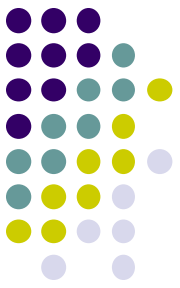
Damping rate of each toroidal mode number n (n=0, 4, 8, 12, 16)

$$\gamma_{d\,n} = D_n / 2E_4$$

Total damping rate of all the toroidal mode numbers (n=0, 4, 8, 12, 16)

$$\gamma_{d\,ALL} = \sum_n D_n / 2E_4$$

Evolution of total damping rate

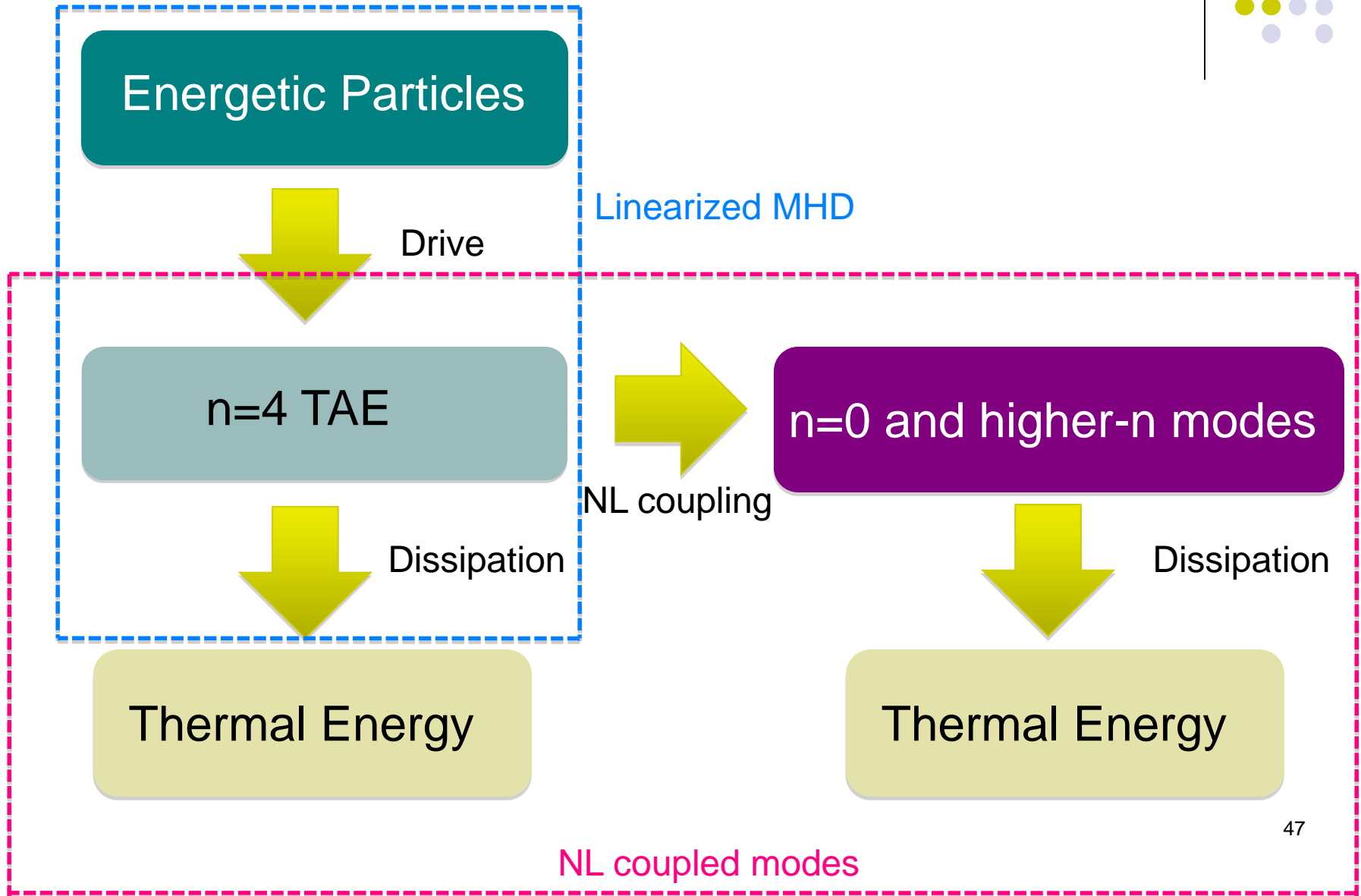β_{h0}=1.7%
Sat. Level (linear) ~ 1.2x10^{-2}
Sat. Level (NL)   ~ 6x10^{-3}
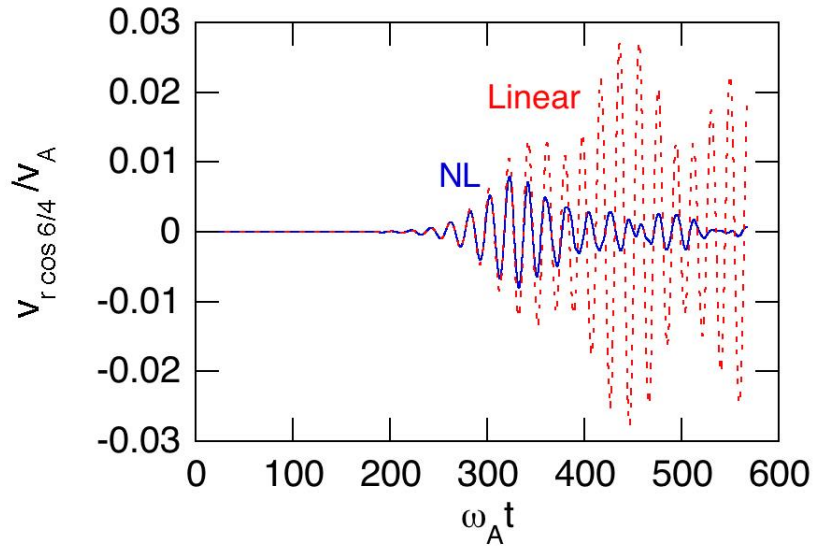
The total damping rate (γ_{dALL}) is greater than the damping rate in the linearized MHD simulation ($\gamma_{d\,lin}$).

Schematic Diagram of Energy Transfer

Energetic Particles

Drive

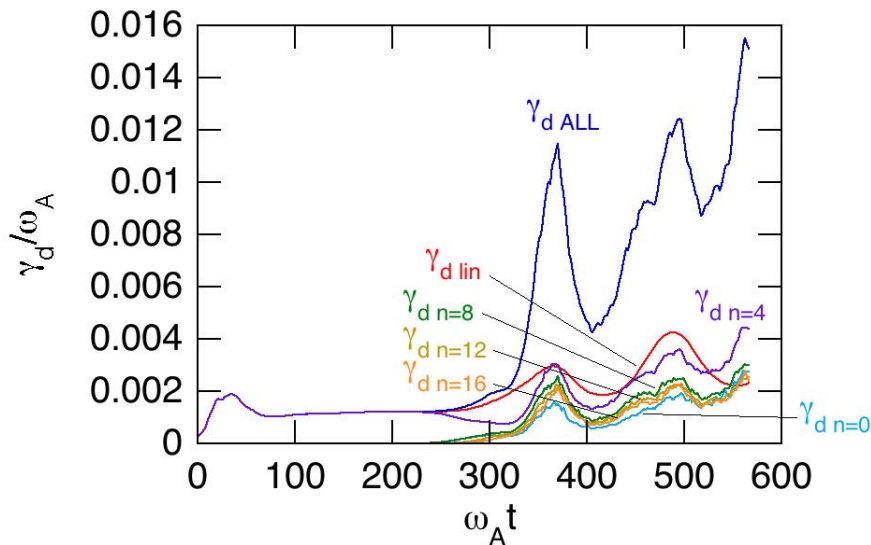Linearized MHD

n=4 TAE → n=0 and higher-n modes

NL coupling

Dissipation

Dissipation

Thermal Energy

Thermal Energy

47

NL coupled modes

Effects of weak dissipation

β_{h0}=1.7%
The viscosity and resistivity are reduced to 1/16,
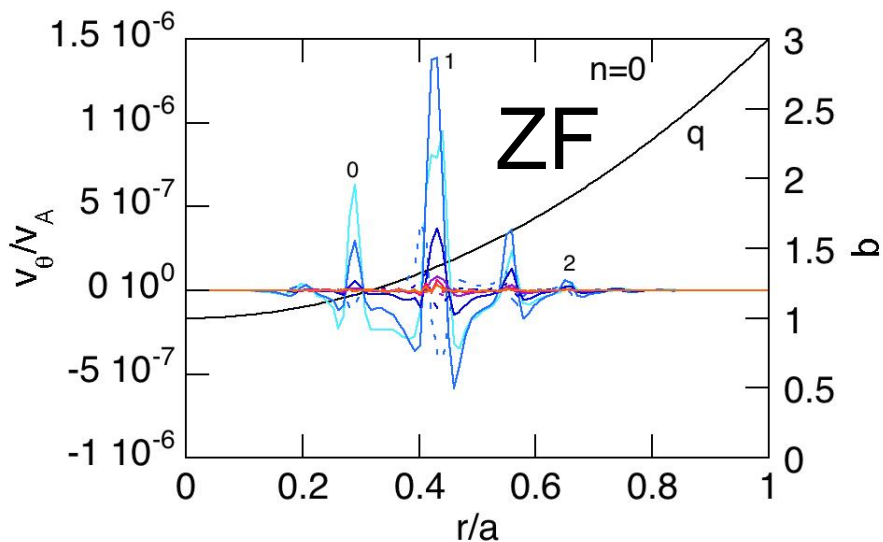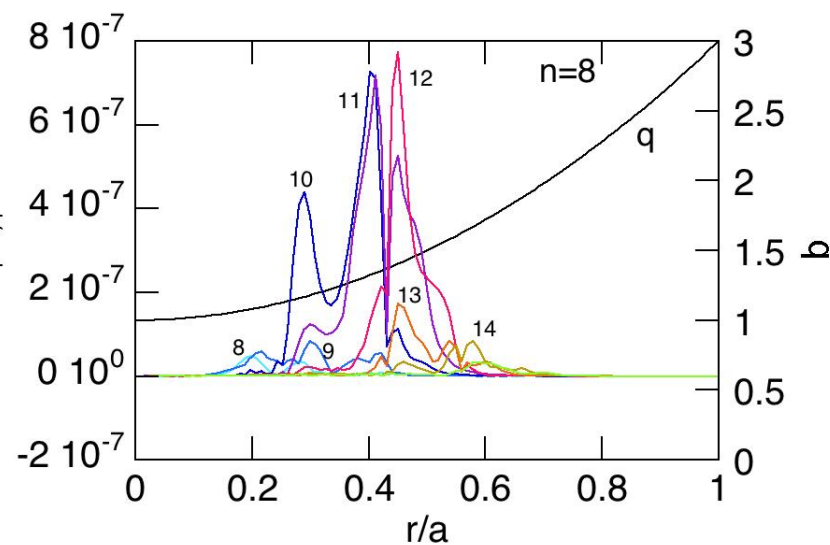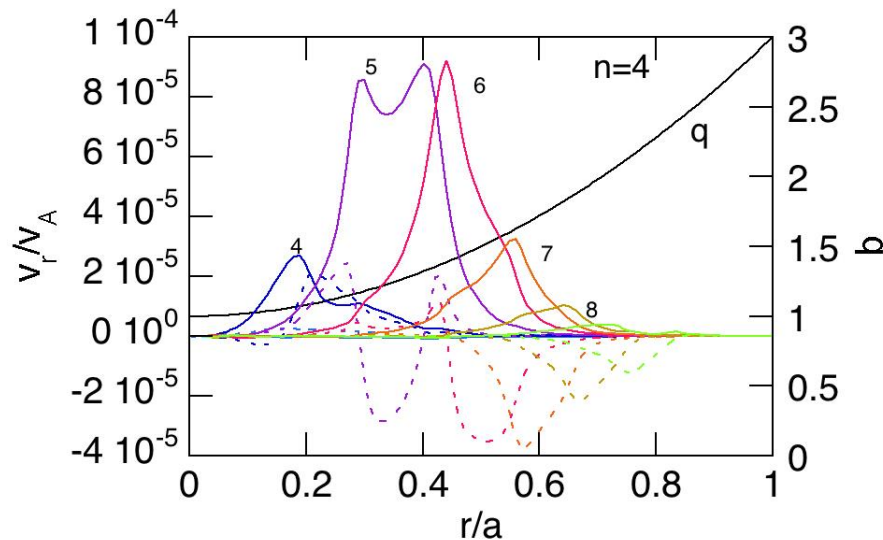$\nu=\nu_n$=6.25 × 10^{-8}v$_A$R$_0$ and
η=6.25 × 10^{-8}μ_0v$_A$R$_0$
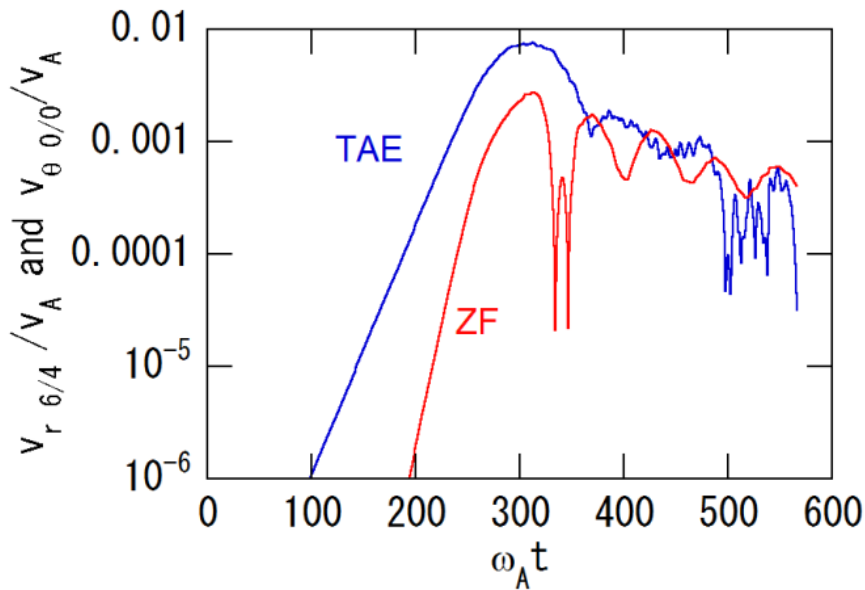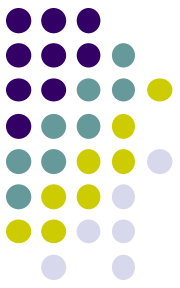with the numbers of grids (512, 512, 128).

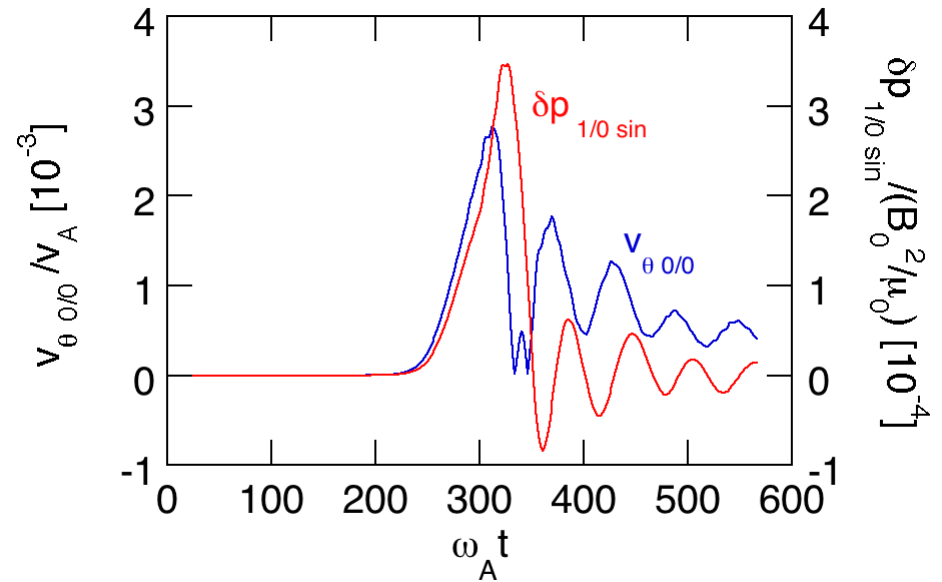The nonlinear MHD effects reduce the saturation level also for weak dissipation.

Spatial profiles of the TAE and NL modes: Evidence for continuum damping of the higher-n (n=8) mode
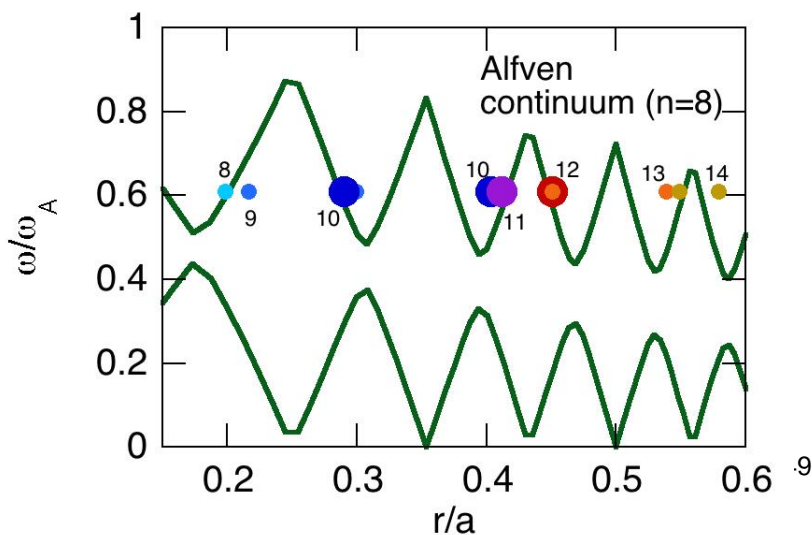
ZF Evolution and GAM Excitation

Evolution of TAE and zonal flow

After the saturation of the TAE instability, a geodesic acoustic mode is excited.

Summary of NL MHD effects on a TAE instability

- Linear and nonlinear simulation runs of a n=4 TAE evolution were compared. The saturation level is reduced by the nonlinear MHD effects.

- The total energy dissipation is significantly increased by the nonlinearly generated modes. The increase in the total energy dissipation reduces the TAE saturation level. The dissipation from higher-n modes can be attributed to the continuum damping.

- The zonal flow is generated during the linearly growing phase of the TAE instability. The geodesic acoustic mode (GAM) is excited after the saturation of the instability. The GAM is not directly excited by the energetic particles but excited through MHD nonlinearity.

SIMULATION OF ALFVÉN EIGENMODE BURSTS WITH NONLINEAR MHD EFFECTS

Comparison between linear and NL MHD runs (j_h' is restricted to n=4)

$$\frac{\partial \rho}{\partial t} = -\nabla \cdot (\rho_{eq}\mathbf{v}) + \nu_n \Delta(\rho - \rho_{eq})$$

$$\rho_{eq}\frac{\partial}{\partial t}\mathbf{v} = -\nabla p + (\mathbf{j}_{eq} - \mathbf{j}'_{heq}) \times \delta\mathbf{B} + (\delta\mathbf{j} - \delta\mathbf{j}'_h) \times \mathbf{B}_{eq}$$

$$+\frac{4}{3}\nabla(\nu\rho_{eq}\nabla \cdot \mathbf{v}) - \nabla \times (\nu\rho_{eq}\omega)$$

$$\frac{\partial \mathbf{B}}{\partial t} = -\nabla \times \mathbf{E}$$

$$\frac{\partial p}{\partial t} = -\nabla \cdot (p_{eq}\mathbf{v}) - (\gamma-1)p_{eq}\nabla \cdot \mathbf{v} + \nu_n \Delta(p - p_{eq})$$

$$+\eta\delta\mathbf{j} \cdot \mathbf{j}_{eq}$$

$$\mathbf{E} = -\mathbf{v} \times \mathbf{B}_{eq} + \eta(\mathbf{j} - \mathbf{j}_{eq})$$

$$\mathbf{j} = \frac{1}{\mu_0}\nabla \times \mathbf{B}$$

$$\omega = \nabla \times \mathbf{v}$$

$$\frac{\partial \rho}{\partial t} = -\nabla \cdot (\rho\mathbf{v}) + \nu_n \Delta(\rho - \rho_{eq})$$

$$\rho\frac{\partial}{\partial t}\mathbf{v} = -\rho\omega \times \mathbf{v} - \rho\nabla(\frac{v^2}{2}) - \nabla p + (\mathbf{j} - \mathbf{j}'_h) \times \mathbf{B}$$

$$+\frac{4}{3}\nabla(\nu\rho\nabla \cdot \mathbf{v}) - \nabla \times (\nu\rho\omega)$$

EP effects

$$\frac{\partial \mathbf{B}}{\partial t} = -\nabla \times \mathbf{E}$$

$$\frac{\partial p}{\partial t} = -\nabla \cdot (p\mathbf{v}) - (\gamma-1)p\nabla \cdot \mathbf{v} + \nu_n \Delta(p - p_{eq})$$

$$+(\gamma-1)[\nu\rho\omega^2 + \frac{4}{3}\nu\rho(\nabla \cdot \mathbf{v})^2 + \eta\mathbf{j} \cdot (\mathbf{j} - \mathbf{j}_{eq})]$$

$$\mathbf{E} = -\mathbf{v} \times \mathbf{B} + \eta(\mathbf{j} - \mathbf{j}_{eq})$$

$$\mathbf{j} = \frac{1}{\mu_0}\nabla \times \mathbf{B}$$

$$\omega = \nabla \times \mathbf{v}$$

The viscosity and resistivity are $\nu = \nu_n = 2 \times 10^{-7} v_A R_0$ and $\eta = 2 \times 10^{-7}\mu_0 v_A R_0$. The numbers of grid points are (128, 64, 128) for (R, φ, z). The number of marker particles is 5.2×10^5.

Simulation with source, loss, collisions and NL MHD

- Time dependent f_0 is implemented in MEGA
- particle loss (at r/a=0.8 for the present runs)
  - for marker particles to excurse outside the loss boundary and return back to the inside
  - phase space inside the loss boundary is well filled with the marker particles
  - particle weight is set to be 0 during r/a>0.8
  - if the simulation box is extended to include the vacuum region, the loss boundary can be set at more realistic location

δf method with time-dependent f₀ (1/2)

$$\frac{\partial}{\partial t} f + \{f, H\} - \nu \frac{\partial}{v^2 \partial v}\left[\left(v^3 + v_c^3\right)f\right] = S(v)$$

When f_0 satisfies

$$\frac{\partial}{\partial t} f_0 + \{f_0, H_0\} - \nu \frac{\partial}{v^2 \partial v}\left[\left(v^3 + v_c^3\right)f_0\right] = S(v) \ ,$$
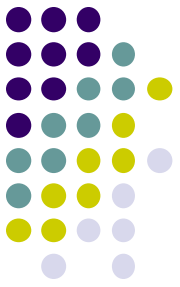
the evoution of δf is given by

$$\frac{\partial}{\partial t} \delta f + \{\delta f, H_0 + H_1\} + \{f_0, H_1\} - \nu \frac{\partial}{v^2 \partial v}\left[\left(v^3 + v_c^3\right)\delta f\right] = 0 \ .$$

With a definition $\dfrac{d}{dt} \delta f \equiv \dfrac{\partial}{\partial t} \delta f + \{\delta f, H_0 + H_1\} - \nu v\left(1 + \dfrac{v_c^3}{v^3}\right)\dfrac{\partial}{\partial v} \delta f,$

the evoution of δf is expressed by

$$\frac{d}{dt} \delta f + \{f_0, H_1\} - 3\nu\delta f = 0 \ .$$

δf method with time-dependent f₀ (2/2)

The evolution of phase space volum V that each particle occupies should be considered. Comparison of two eqs.:

$$\frac{d}{dt}\left(fV\right) = SV$$

and

$$\frac{d}{dt}f - 3vf = S$$

gives

$$\frac{d}{dt}V = -3vV$$

We solve the evolution of both δf and V of marker particles.

Time-dependent f_0

A solution of

$$\frac{\partial}{\partial t} f_0 - \nu \frac{\partial}{\mathrm{v}^2 \partial \mathrm{v}}\left[\left(\mathrm{v}^3 + \mathrm{v}_c^3\right) f_0\right] = S(\mathrm{v}) \,,$$

is

$$f_0(\mathrm{v}, t) = \frac{1}{\nu}\,\frac{1}{\mathrm{v}^3 + \mathrm{v}_c^3}\left[\mathrm{erf}\left(\frac{\mathrm{v'} - \mathrm{v}_b}{\Delta\mathrm{v}}\right) - \mathrm{erf}\left(\frac{\mathrm{v} - \mathrm{v}_b}{\Delta\mathrm{v}}\right)\right]$$

with

$$\mathrm{v'} = \left[\left(\mathrm{v}^3 + \mathrm{v}_c^3\right)\exp\left(3\nu(t + t_{inj})\right) - \mathrm{v}_c^3\right]^{1/3} \,,$$

$$S(\mathrm{v}) = \frac{2}{\sqrt{\pi}}\,\frac{1}{\mathrm{v}^2 \Delta\mathrm{v}}\exp\left[-\left(\frac{\mathrm{v} - \mathrm{v}_b}{\Delta\mathrm{v}}\right)^2\right] \,,$$

$\mathrm{v}_b :$ injection or birth velocity of energetic particle

$t_{inj} :$ injection starts at $t = -t_{inj} < 0$

Note :

Here we have neglected $\{f_0, H_0\}$ term

for parallel beam injection

(zero magnetic moment)

and w/o finite orbit width effect.

Physics condition

- similar to the reduced simulation of TAE bursts at the TFTR experiment

- parameters

  - $a=0.75m$, $R_0=2.4m$, $B_0=1T$, $q(r)=1.2+1.8(r/a)^2$

  - NBI power: 10MW

  - beam injection energy: 110keV (deuterium)

  - $v_b=1.1v_A$

  - parallel injection ($v_{//}/v=-1$ or 1)

  - slowing down time: 100ms

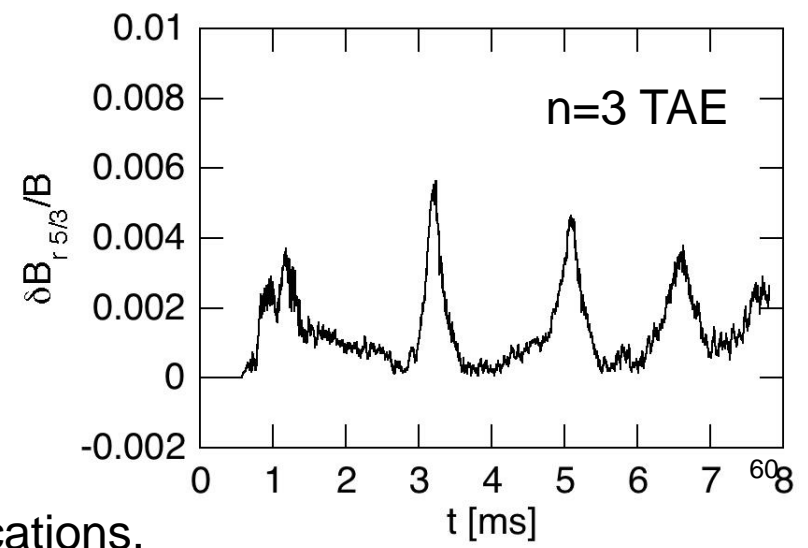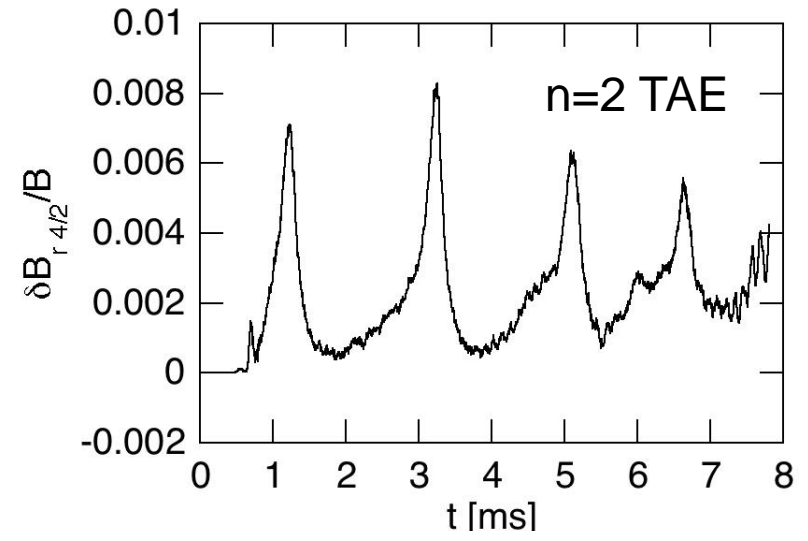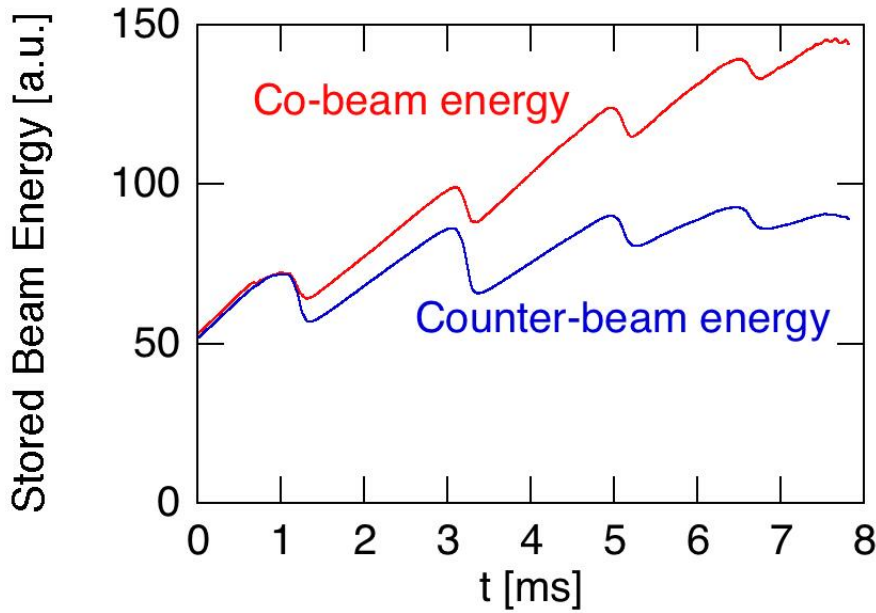 - no pitch angle scattering

TAE mode spatial profiles
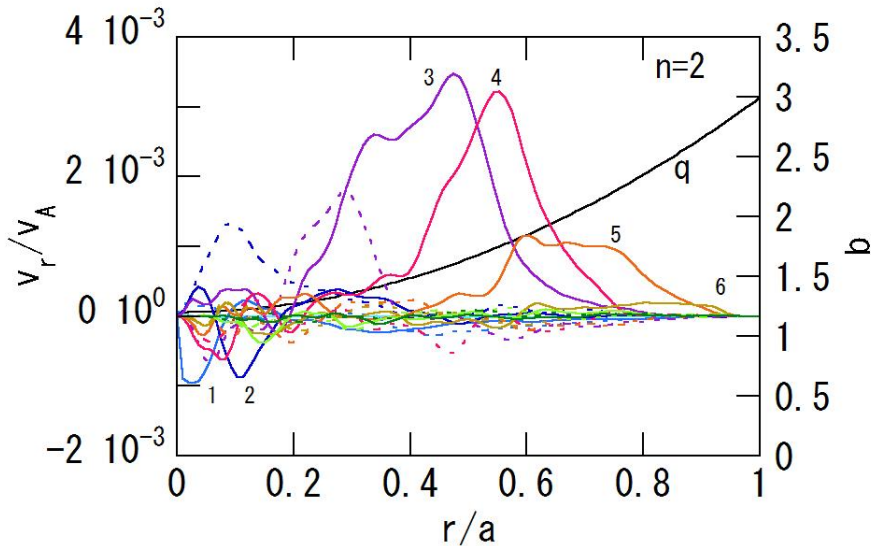
- n=2 TAE mode profile
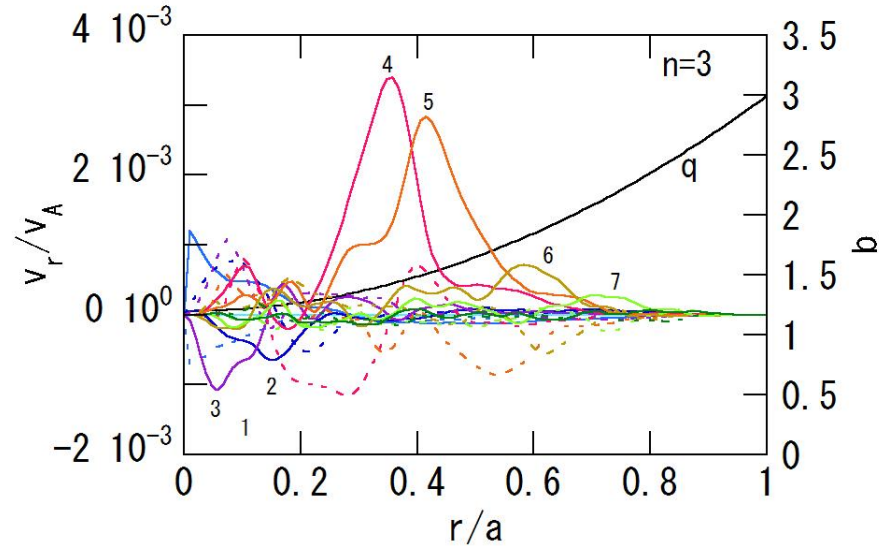
- n=3 TAE mode profile

Evolution of stored beam energy and TAE amplitude

- Energetic particle losses due to TAE bursts.
- Synchronization of multiple TAEs.

■ $\nu = \eta/\mu_0 = \chi = 2 \times 10^{-7} v_A R_0$
■ Amplitude is measured at the mode peak locations.

NL MHD effects

- reduction of saturation level
- suppression of beam ion loss

$\blacksquare$ $\nu = \eta/\mu_0 = \chi = 10^{-7} v_A R_0$

stored beam energy   n=2 TAE peak amplitude

NL MHD

Linear MHD

61
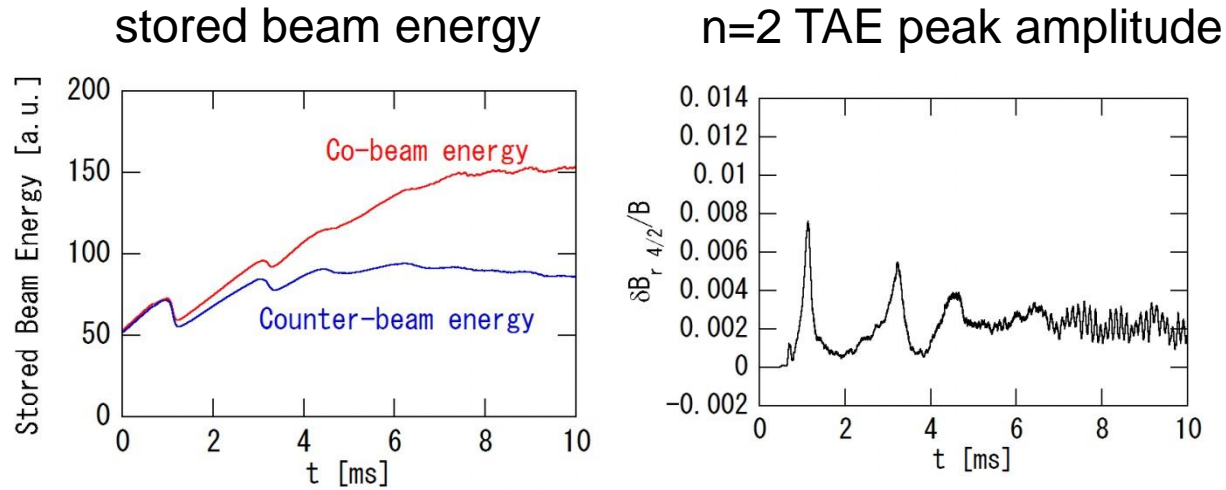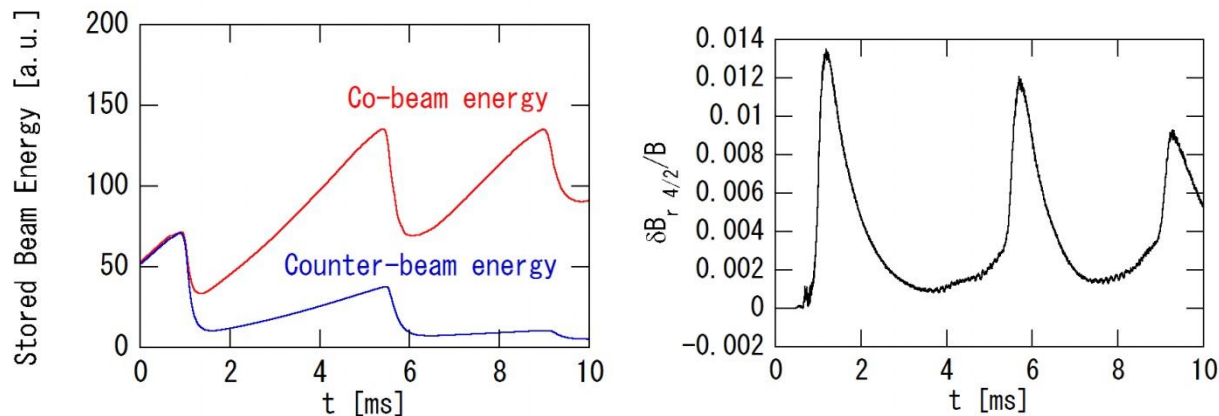
Effects of dissipation coefficients

- Higher dissipation → bursts
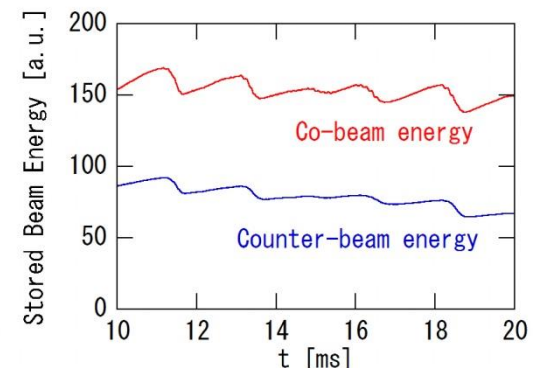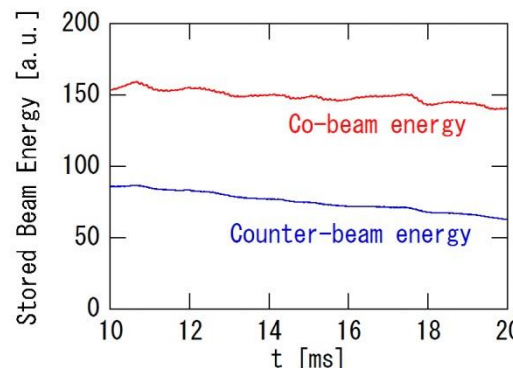
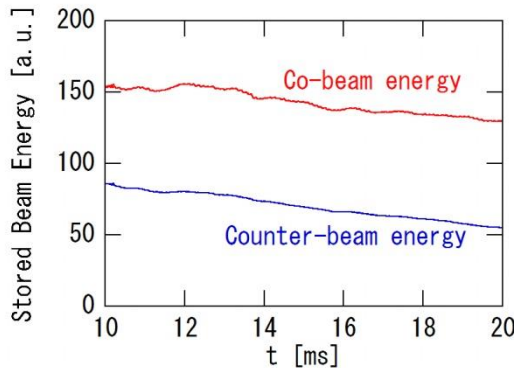■ $\nu = \eta/\mu_0 = \chi = 10^{-7} v_A R_0$ ■ $3 \times 10^{-7} v_A R_0$ ■ $5 \times 10^{-7} v_A R_0$
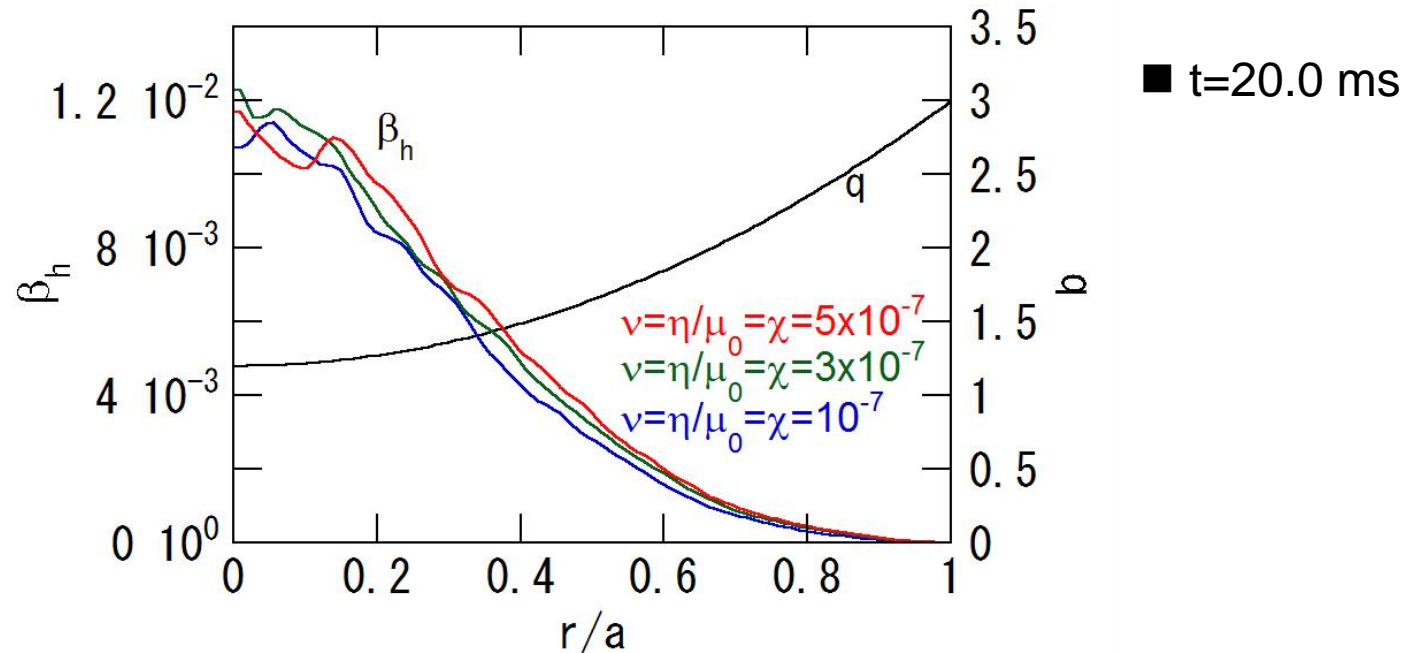
n=2 TAE peak amplitude
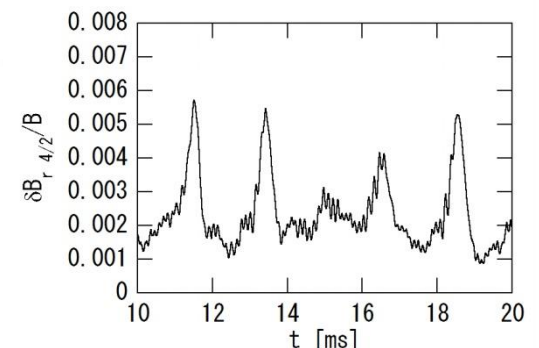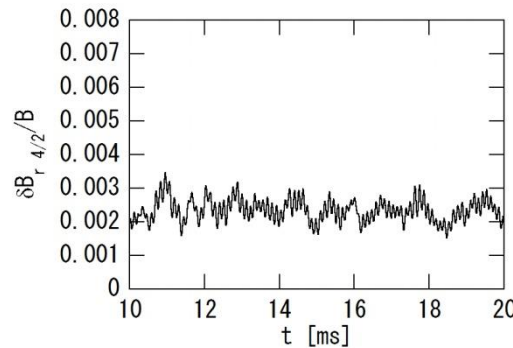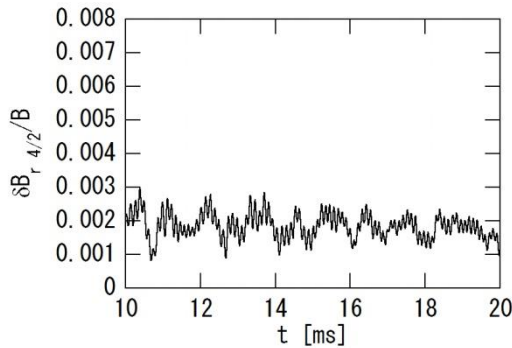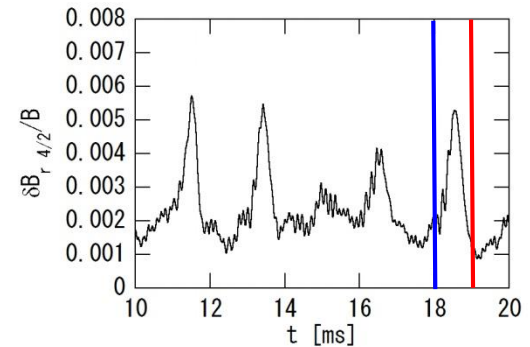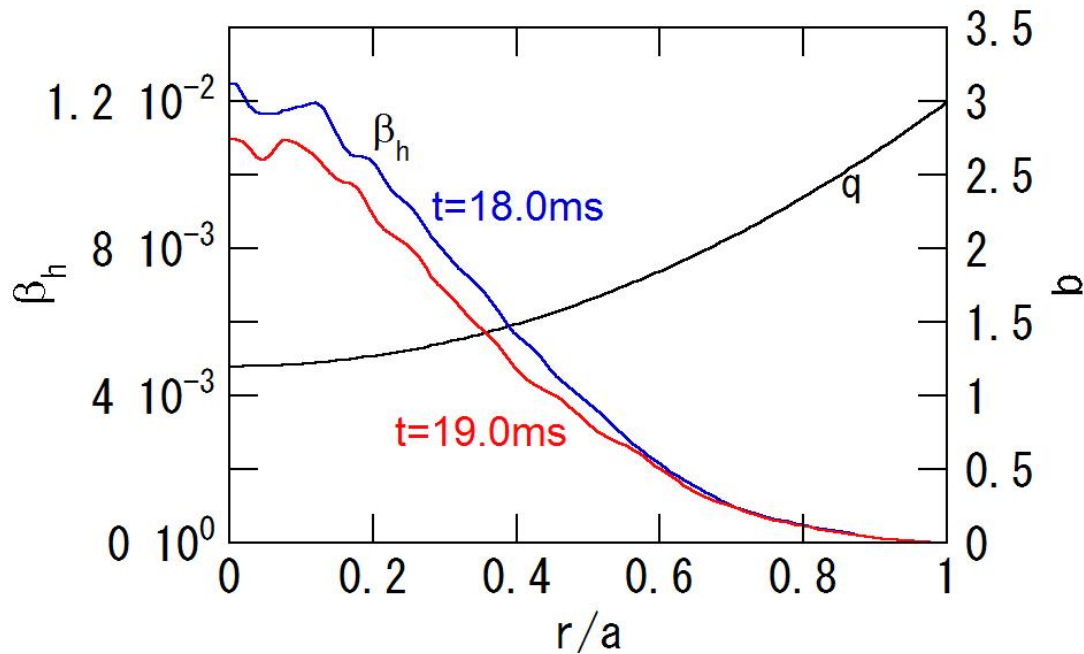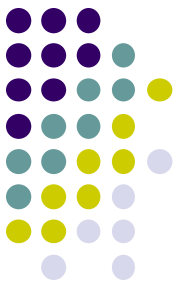
stored beam energy

Comparison of EP pressure profiles for different dissipation

■ t=20.0 ms

■ EP pressure profiles are very similar among the different dissipation coefficients.

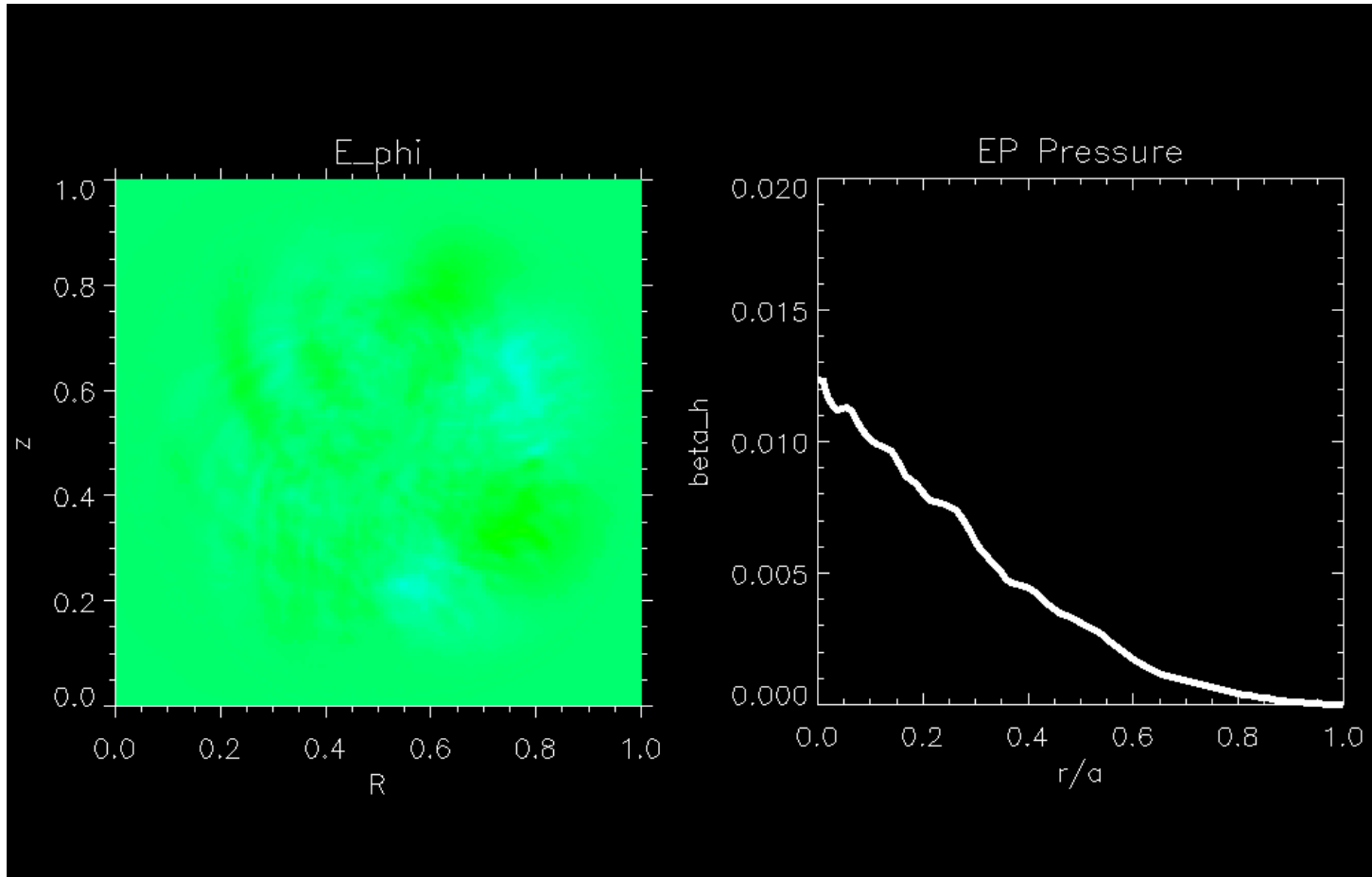■ Higher dissipation leads to slightly higher EP pressure.

63

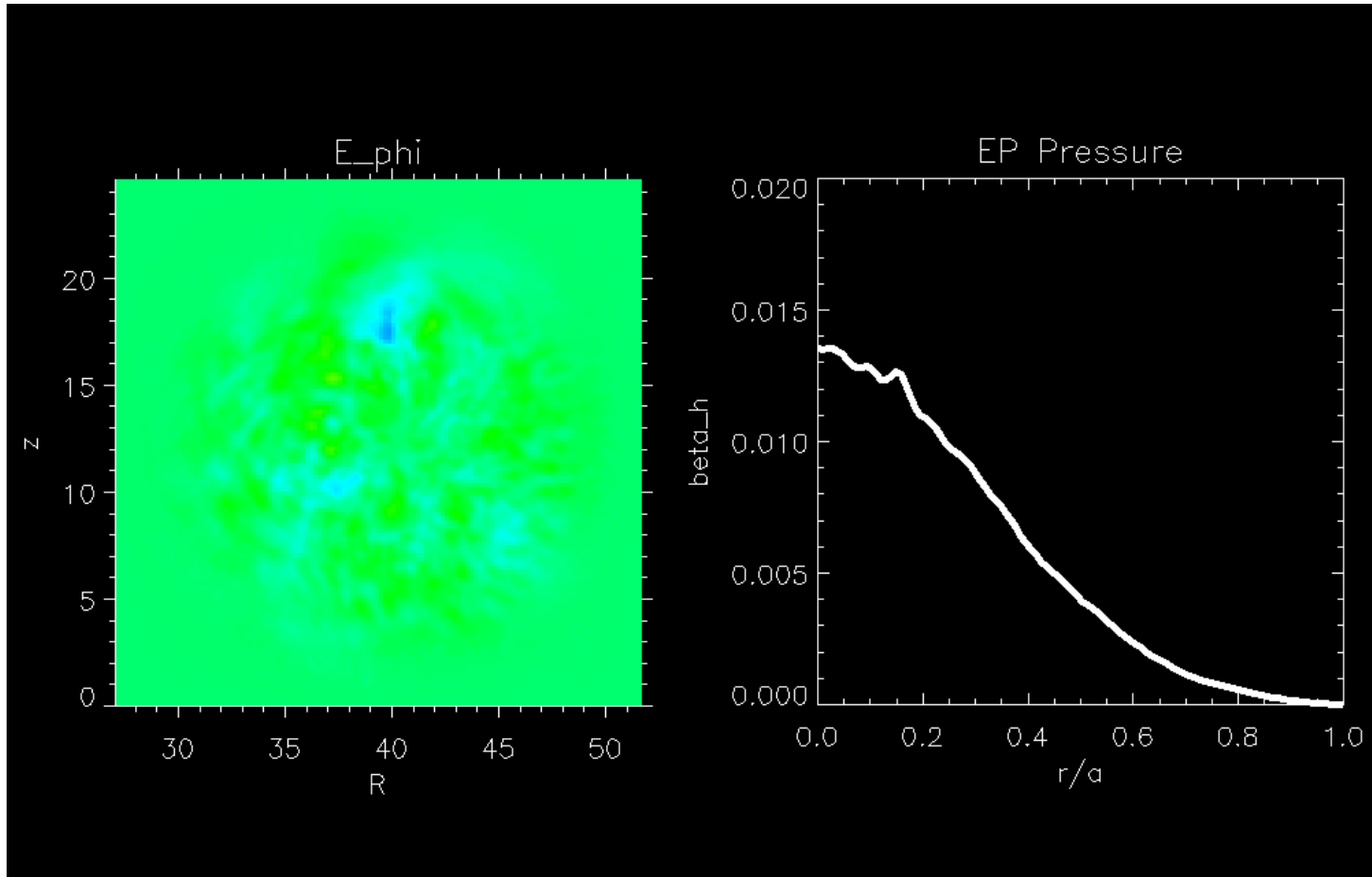# Comparison of EP pressure profiles before and after a burst

$\nu = \eta/\mu_0 = \chi = 5 \times 10^{-7} v_A R_0$

■ EP transport and losses during the TAE burst lead to a reduction in pressure profile.

Linear MHD

Nonlinear MHD

Summary of TAE burst simulation with NL MHD effects

- TAE bursts are successfully simulated with NL MHD effects using time-dependent f_0.

  - saturation amplitude of the dominant harmonic with significant beam ion loss: $\delta B/B \sim 5 \times 10^{-3}$

- NL MHD effects

  - reduction of saturation level

  - suppression of beam ion loss

- Effects of dissipation

  - Low dissipation: statistically steady state

  - High dissipation: bursts

  - Higher dissipation leads to higher stored beam energy

Outline

- Introduction
  - Interaction of energetic particles and Alfvén eigenmode in toroidal plasmas
- Simulation models
  - EP + MHD hybrid simulation model
  - Reduced simulation model with constant AE spatial profile
- Simulation of AE bursts
  - Reduced simulation
  - Hybrid simulation with nonlinear MHD effects